Chapter 5
Formulation and development: Vinorelbine tartrate

5.0 MATERIALS AND METHODS

5.1 Materials

Vinorelbine Tartrate (VBT) was obtained as gift sample from Cipla Limited, Mumbai, India. Human Serum Albumin (HSA) fraction V (purity 96–99%, 65,000 Da), and 8% aqueous glutaraldehyde solution were purchased from Sigma Aldrich, Germany. Sodium Chloride (NaCl) was purchased H. B. Chemicals, Vadodara, India. Cellulose dialysis tubing (Molecular weight cut of 12000) and membrane filter of pore size 0.2 µm were purchased from Himedia Lab, Mumbai, India. All other chemicals and reagents used in this study were of analytical grade.

5.2 Equipments

- Digital Analytical Balance (Shimadzu SCS, Switzerland)
- High Speed Magnetic Stirrer (Remi, MS500, Remi equipments, Mumbai, India)
- High Speed Centrifuge (Sigma 3K30, Germany)
- Particle Size Analyzer 3000 HS (Zeta sizer Nano series, Malvern Instruments, UK)
- Lyophilizer (Heto, Vaccubrand, Denmark)
- Differential Scanning Calorimeter (Mettler Toledo DSC 822e, Japan)
- Transmission Electron Microscope (Philips, Technai 20, Holland)

5.3 Preparation of VBT HSA Nanoparticles (VBT-HSA-NPs) by Desolvation

5 to 25 mg of albumin/mL of 10 mM NaCl solution was adjusted to pH 7.0–9.0 and then 0.5–2.5 mg/mL vinorelbine was added. The mixed solution was transformed into NPs by continuous addition of desolvating agent under constant stirring (100-1000 rpm) at room temperature. After the desolvation process, 8% aqueous glutaraldehyde solution was added to induce particle cross-linking (the amount of glutaraldehyde is equal to 50% and 150% of calculated amount necessary for the quantitative cross-linking of the 59 amino groups in the serum albumin molecule). The cross-linking process was performed under constant stirring of the suspension over a time period of 24 h. The resulting NPs were purified by five cycles of centrifugation (15,000 × g, 5 min) and redispersion of the pellet to the original volume with 10 mM NaCl solution. Each redispersion step was performed in an ultrasonication bath over 3 min, in order to remove the organic solvent completely and finally the dispersion was lyophilized (1, 2).

5.4 Preliminary Optimization of Parameters

In preliminary optimization the parameters influencing the formation of NPs were identified and optimized (3). During preliminary optimization after protein desolvation 8% aqueous glutaraldehyde solution was added to induce particle cross-linking. Glutaraldehyde concentration was chosen to 100% of the theoretical amount that is necessary for the quantitative cross-linking of the amino groups in the HSA molecule (4).

5.4.1 Optimization of Formulation Parameters

Formulation parameter optimization such as VBT: HSA ratio, and Concentration of VBT were optimized for desired results. Effect of one variable was studied at a time keeping other variables constant.

5.4.1.1 VBT: HSA ratio

Optimized on the basis of particle size and percent entrapment of the NPs formed at different VBT: HSA ratio. Numbers of trials were carried out at different VBT: HSA ratio (1:5, 1:10 and 1:15) to optimize the ratio forming uniform NPs.

5.4.1.2 Concentration of VBT

Optimized on the basis of particle size and percent entrapment of VBT in NPs formed at different concentration of VBT in the formulation. Numbers of trials were carried out at different concentration of VBT (0.5-5.0 mg/ml) to optimize the concentration forming uniform NPs.

5.4.2 Optimization of Process Parameters

Process parameter optimization such as concentration and type of the desolvating agents, stirring rate and addition system of desolvating agent were optimized for desired results. Effect of one variable was studied at a time keeping other variables constant.

5.4.2.1 Concentration and type of the desolvating agents

The effect of various concentration and type of the desolvating agents on formation of NPs was optimized. Desolvating agents along with their volume and concentration used for protein desolvation given in **Table 5.1.** Non desolvated percentage of protein after desolvation was determined after separating the NPs from

the aqueous supernatant (containing non-entrapped VBT) by centrifugation at 25000 rpm for 30 min. The amount of protein dissolved in the supernatant was determined using a standard BCA protein assay. To 0.3 ml of the supernatant 8 ml of the BCA working reagent was added. After incubating the mixture at 30°C for 60 min the samples were analyzed spectrophotometrically at 562 nm. The protein content of the samples was calculated relative to reference.

Table 5. 1 Amount and concentration desolvating agents used for protein desolvation

Desolvating agent	Concentration (m/m %)	Amount used (mL)
Ethanol/water	95, 90, 80, 70	5
Methanol/water	100, 90, 80, 70	10
Acetone/water	90, 80, 70, 60	5

Mass percent (m/m) = The mass of solute in grams for exactly 100 g of solution.

5.4.2.2 Stirring Rate

The preparation of HSA NPs was performed at different stirring rates (200–1000 rpm) during desolvation process. For these experiments, ethanol 70 % (m/m) was used as desolvating agents.

5.4.2.3 Addition system of desolvating agent

The influence of continuous addition of the desolvating agent was compared to the drop wise addition. Under all process conditions, the resulting particle systems were stabilized by the addition of an 8% aqueous glutaraldehyde solution leading to a cross-linking of the particle matrix. The continuous addition was performed by placing the end of the tube containing the desolvating agent below the surface of the protein solution, so that no drop-formation was possible, resulting in a homogeneous distribution of the desolvating agent.

5.5 Optimization of VBT-HSA-NPs by Central Composite Design (CCD)

In response surface methodology (RSM) (5) the experimentation is completed before the optimization takes place. In RSM methods, one or more selected experimental responses are recorded for a set of experiments carried out in a systematic way to predict the optimum and the interaction effects (6). In this study based on the benefit and published literatures on CCD (7), it was selected as optimization design for

optimization of albumin NPs by desolvation method. For nonlinear responses requiring second-order models, central composite designs (CCDs) are the most frequently employed and is also known as the Box–Wilson design, the "composite design" contains an imbedded (2^k) FD or (2^{k-r}) FFD, augmented with a group of star points (2^k) and a "central" point (8). The star points allow estimation of curvature and establish new extremes for the low and high settings for all the factors. Hence, CCDs are second-order designs that effectively combine the advantageous features of both FDs (and FFDs) and the star design shown in **Figure 5.1**.

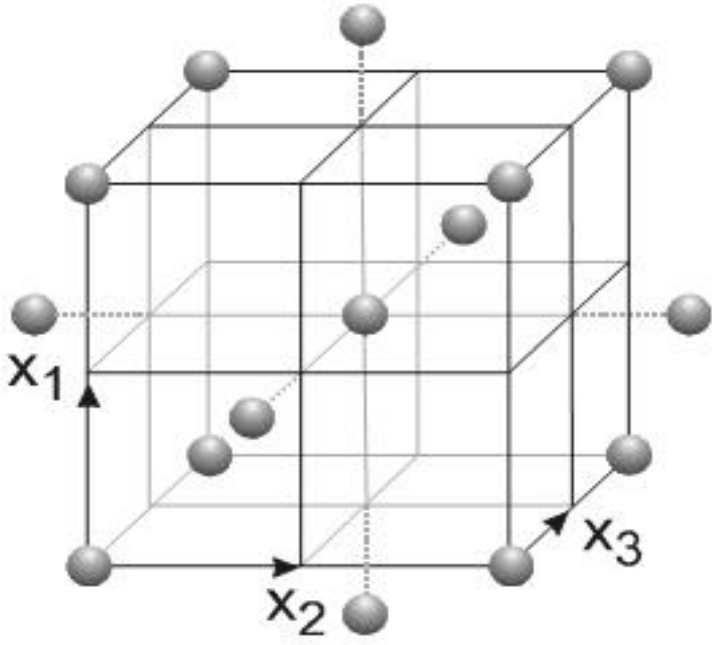

Figure 5. 1 Diagrammatic representation of a CCD

The total number of factor combinations in a CCD is given by $2^k + 2k + 1$. Preliminary studies were undertaken to decide the excipients and their levels in experimental design. For the RSM involving CCD, a total 30 experiments were conducted for four factors at five levels. Factors that might affect the designed characteristic of NP formulation were varied over five levels given in **Table 5.2** and formulations were arranged according to a CCD given in **Table 5.3.**

Mathematical model was developed for optimization of NPs by CCD in order to deduce the adequate conditions to prepare albumin NPs by desolvation method of desired characteristics. Response surface methodology combined with CCD was used to generate the relationship between the independent variables and dependent variables

(9). A four-factor, five-level CCD with six replicates at the center point was selected to build response surface models. The design and statistical analysis were performed by Design Expert® Software (Version 8.0.7.1, Stat-Ease Inc, Minneapolis, USA) for design of experiments (DOE).

Based on the preliminary experiment three factors the albumin concentration (mg/ml) (X_1), vinorelbine amount (mg) (X_2), pH (X_3) and glutaraldehyde concentration (X_4) were selected as independent variables and the particle size (Y_1) and % entrapment efficiency (% EE) (Y_2) were selected as dependent variables (responses). Factors that might affect the designed characteristic of NP formulations were varied over five levels given in **Table 5.2** and five-level CCD was developed to explore the optimum levels of these variables. This methodology consisted of different groups of design points including factorial design points, axial or star points, and center points. Formulations were arranged according to a CCD are given in **Table 5.3.**

Table 5. 2 Factors and levels of factors studied in a CCD

Independent Variable	**Coded Levels**				
	-2	-1	0	+1	+2
Albumin concentration in mg/ml (X_1)	5	10	15	20	25
Vinorelbine in mg (X_2)	0.5	1	1.5	2	2.5
pH (X_3)	7.0	7.5	8.0	8.5	9.0
Glutaraldehyde Concentration in % (X_4)	50	75	100	125	150

Table 5. 3 CCD Experimental Layout

Formulation Code	Run	Point Type	Independent Variables			
			A	B	C	D
F 1	15	Factorial	10	1.5	7.5	75
F 2	5	Factorial	20	1.5	7.5	75
F 3	2	Factorial	10	1.5	7.5	75
F 4	18	Factorial	20	1.5	7.5	75
F 5	22	Factorial	10	1.5	8.5	75
F 6	8	Factorial	20	1.5	8.5	75
F 7	6	Factorial	10	1.5	8.5	75
F 8	27	Factorial	20	1.5	8.5	75
F 9	1	Factorial	10	2.5	7.5	125
F 10	7	Factorial	20	1.5	7.5	125
F 11	20	Factorial	10	0.5	7.5	125
F 12	3	Factorial	20	1.5	7.5	125
F 13	26	Factorial	10	1.5	8.5	125
F 14	9	Factorial	20	1.5	8.5	125
F 15	10	Factorial	10	1.0	8.5	125
F 16	17	Factorial	20	2.0	8.5	125
F 17	12	Axial	5	2.0	8.0	100
F 18	29	Axial	25	1.0	8.0	100
F 19	24	Axial	15	2.0	8.0	100
F 20	13	Axial	15	1.0	8.0	100
F 21	11	Axial	15	1.0	7.0	100
F 22	25	Axial	15	1.0	9.0	100
F 23	30	Axial	15	2.0	8.0	50
F 24	21	Axial	15	1.0	8.0	150
F 25	19	Center	15	2.0	8.0	100
F 26	28	Center	15	2.0	8.0	100
F 27	14	Center	15	2.0	8.0	100
F 28	16	Center	15	1.0	8.0	100
F 29	4	Center	15	1.0	8.0	100
F 30	23	Center	15	2.0	8.0	100

5.5.1 Optimization Data Analysis

Various RSM computations for the current optimization study were performed and polynomial models including interaction and quadratic terms were generated for the response variables using multiple regression analysis (MLRA) approach (6).

A second degree polynomial model for this response is as follows:

$$\mathbf{Y} = \beta_0 + \beta_1 X_1 + \beta_2 X_2 + \beta_3 X_3 + \beta_{12} X_1 X_2 + \beta_{13} X_1 X_3 + \beta_{14} X_1 X_4 + \beta_{23} X_2 X_3 + \beta_{24} X_2 X_4 + \beta_{34} X_3 X_4 + \beta_{11} X^2_1 + \beta_{22} X^2_2 + \beta_{33} X^2_3 + \beta_{44} X^2_4$$

Where Y = measured response associated with each factor level combination; β_0 = intercept; β_1 to β_{33} are regression coefficients computed from the observed experimental values of Y from experimental runs; and X_1, X_2, X_3 and X_4 are the coded levels of independent variables. The polynomial equation was used to draw conclusions after considering the magnitude of coefficients and the mathematical sign it carries, i.e. positive sign indicates the synergistic effect, whereas a negative sign indicates the antagonistic effect. By using this equation, it is possible to evaluate appropriately the linear, quadratic and interactive effects of the independent variables on the responses. The statistical analysis of the data through regression model and plotting the response surface graphs were carried out using Design-Expert. Analysis of variance (ANOVA) evaluated the significance of each coefficient by p-value (less than 0.05) through Fisher's test and it helps to choose the significant model (10). The predicted values and the experimental parameters were evaluated by the correlation coefficient and the adjusted correlation coefficient. In order to find the optimized formulations, in all experimental regions the numerical searches were employed by considering the constraints in which the particle size is in its minimum level and % EE is in its maximum level. The experimental responses were compared with the predicted values (obtained from the equation) to evaluate the precision of the model.

5.5.2 Response Surface Plots

Response surface plots were used as a function of two factors at a time maintaining all other factors at fixed levels to understand the main and interaction effects of two variables (11). These plots were obtained by calculating the values taken by one factor where the second varies (from -1 to 1 for instance) with constraint of a

given Y value. The yield values for different levels of variables can also be predicted from the respective response surface plots.

5.5.3 Validation of Optimization Methodology (Check Point Analysis)

Validation of the optimization methodology (12) is a very crucial step that tells about the prognostic ability of the model studied. So the generated polynomials are tested for their predictive abilities. The predicted values are compared with that of the observed experimental data and the percentage residual error is determined. Various new batches of VBT-HSA-NPs were prepared experimentally by taking the amounts of the independent variables (X_1 and X_2) selected from the different regions of the experimental domain and evaluated according to the standard operating conditions. Each batch was prepared three times and mean values were determined. Difference in the predicted and mean values of experimentally obtained particle size, and % EE was compared.

5.5.4 Desirability Criteria

For simultaneous optimization of particle size and % EE, desirability function was applied and total desirability was calculated using Design Expert software. The desirability lies between 0 and 1 and it represents the closeness of a response to its ideal value (13). If both the quality characteristics reach their ideal values, the individual desirability is 1. Consequently, the total desirability is also 1. Our optimization criteria included minimum particle size and maximum % EE.

5.6 Lyophilization of VBT-HSA-NPs

The optimized NP formulation was lyophilized without any cryoprotectant (14). Nanoparticulate suspension (3 ml) was dispensed in 10 ml semi-stoppered vials with rubber closures and frozen for 24 h at -70 °C. Thereafter, the vials were lyophilized in lyophilizer. Finally, glass vials were sealed and stored until being re-hydrated. Lyophilized NPs were re-dispersed in exactly the same volume of distilled water as before lyophilization and were evaluated for particle size and % drug content.

5.7 Characterization of VBT-HSA-NPs

VBT-HSA-NPs were characterized for different parameters as mentioned below.

5.7.1 Particle Size

The size analysis and polydispersity index of the NPs were determined using a Malvern Zetasizer. Each sample was diluted ten times with filtered double distilled water to avoid multi-scattering phenomena and placed in disposable sizing cuvette. Polydispersity index was noted to determine the narrowness of the particle size distribution. The size analysis was performed in triplicate and the results were expressed as mean ± SD.

5.7.2 Zeta Potential

Zeta potential was measured using a Malvern Zetasizer at 25°C. Each sample was suitably diluted 10 times with filtered double distilled water and placed in a disposable zeta cell. The electrophoretic mobility (µm/sec) was converted to zeta potential by in-built software using Helmholtz-Smoluchowski equation. The measurements were performed in triplicate.

5.7.3 % Entrapment Efficiency (% EE)

The % EE was determined after separating the NPs from the aqueous supernatant (containing non-entrapped VBT) by centrifugation at 25000 rpm for 30 min. The supernatant was diluted with appropriate amount of distilled water and analyzed for the amount of unentrapped drug by HPLC after filtration through 0.22 µ. The HPLC system comprised of a pump and UV Vis detector with a C18 column (Particle size 10 µm, 4.6 mm x 250 mm) that was used to elute VBT. The mobile phase was a mixture of acetonitrile and 50 mM phosphate buffer solution containing 1% triethylamine (60/40, v/v; the pH of aqueous phase was adjusted to 4.0 with H3PO4), running at a flow rate of 1 mL/min. Detection was accomplished at 271.2 nm. The samples were chromatographed at 25 °C by injecting 20 µL into the HPLC system. The peak area of VBT was recorded and the concentration of VBT was calculated from a standard curve. The % EE was estimated by calculating amount of drug entrapped in NPs with respect to total drug added during preparation of formulation. The EE was calculated according to following formula:

$$\% EE = (\text{Total amount of drug added- amount of drug in supernatant} / \text{Total amount of drug added}) \times 100$$

5.7.4 Differential Scanning Calorimetry (DSC)

DSC analysis was carried out using a Differential Scanning Calorimeter at a heating rate of 10°C per minute in the range of 30°C to 300°C under inert nitrogen atmosphere at a flow rate of 40 ml/min. DSC Thermograms were recorded for VBT, HSA, VBT-HSA physical mixture and VBT-HSA-NPs.

5.7.5 Transmission Electron Microscopy (TEM)

Transmission Electron Microscopy (TEM) is useful since it allows particles much smaller than 1 µm to be measured. In present work, Transmission Electron Microscopy was performed by Philips Technai 20 instrument. NPs were dispersed in distilled water and drop of redispersed NP was incubated on carbon coated copper grid. This copper grid was fixed into sample holder and placed in vacuum chamber of transmission electron microscope and observed under low vacuum.

5.7.6 *In-vitro* drug release

The *in vitro* drug release was carried out by dialysis bag technique (15). A dialysis membrane MWCO 12000 was used for *in vitro* release studies. 1 ml of formulation (Plain drug dispersion and VBT-HSA-NPs) was placed in dialysis bag. Bag was sealed at both ends and placed in a beaker containing 20 ml of receptor medium (PBS {pH 7.4}). Samples (1 ml) were withdrawn from the receptor compartment at predetermined time intervals, and the volume was replenished with same volume of diffusion medium. Addition of diffusion medium to the receptor compartment was performed with great care to avoid trapping air beneath the diffusion membrane. The samples were diluted and analyzed by HPLC at 271.2 nm. The % drug release was calculated. Graph of % drug release vs. time was plotted. The drug release studies were performed in triplicate.

5.7.7 Stability Studies

The stability of VBT-HSA-NPs in terms of drug content and particle size distribution was monitored for 6 months at 2-8 °C and room temperature. Periodically, samples were withdrawn and the particle size as well as VBT content was determined.

5.8 Results

5.8.1 Preliminary Optimization

5.8.1.1 Optimization of Formulation Parameters

VBT: HSA ratio: The effect of VBT: HSA ratio on particle size and % EE of NPs was observed. Results indicate that at 1:5 VBT: HSA ratio, smaller particle size NPs were obtained but % EE was low. At 1:10 VBT: HSA ratio the particle size of NPs was minimum and % EE was highest. As the VBT: HSA ratio increases from 1:10 to 1:15 there was increase in particle size of NPs and decreased % EE was observed may due to higher amount of albumin results are given in **Table 5.4.**

Table 5. 4 Particle size, PDI and % EE at different VBT: HSA ratios

Drug :HSA Ratio	Particle Size of NPs (nm) * (Mean ± SD)	PDI* (Mean ± SD)	% EE*
1:5	165±6.57	0.456±0.048	65 ± 2.357
1:10	172±4.85	0.313±0.075	73 ± 1.144
1:15	185±6.27	0.556±0.064	75 ± 1.532
1:20	234±5.82	0.523±0.085	65 ± 2.746

* The experiment was performed in triplicate (n=3)

Concentration of drug: The effect of various concentrations of VBT on particle size PDI and stability of NPs was observed. Results indicate that at lower concentration of drug (0.5 mg/ml), the particle size of NPs was somewhat large. At intermediate concentration of drug (1-2 mg/ml), the particle size of NPs was minimum and stable NPs were formed may be due to sufficient amount of albumin and glutaraldehyde to stabilize drug loaded NPs. As the concentration of drug increased from 2.5 to 5 mg/ml, there was increase in particle size of NPs and unstable NPs were formed as depicted in **Table 5.5.**

Table 5. 5 Particle size, PDI and stability results at different drug concentration

Concentration of Drug (mg/mL)	Particle size NPs (nm)* (Mean ± S.E.M)	PDI* (Mean ± S.E.M)	Observation
0.5	175±3.86	0.421±0.034	Stable NPs
1	185±5.54	0.281±0.067	Stable NPs
2	254±4.48	0.545±0.078	Stable NPs
2.5	376±7.85	0.365±0.081	Unstable NPs
5	436±6.54	0.478±0.056	Unstable NPs

* The experiment was performed in triplicate (n=3)

5.8.1.2 Optimization of process parameters

Concentration and type of the desolvating agents: The first focus was to evaluate the effect of different desolvating agents on particle size and polydispersity stability of HSA NPs. Acetone as desolvating agent at lower concentrations (60-70 %) led to monodisperse NPs in a size range of about 230 nm whereas at higher concentrations led increase in particle sizes of NPs may be due to agglomeration of particles at higher concentration of acetone. At 90% concentration of acetone, a significant increase of particle size and PDI (365 nm and 0.45) was observed and higher concentrations of acetone led to higher size of NPs (more than 700 nm and microparticles also). Ethanol as desolvating agent at lower concentrations (70-80 %) led to NPs in a size range of 130-185 nm and at 90% concentrations the particle size of NPs was remained approximately constant, while increase in ethanol concentrations up to 95% led to increase in size of NPs. Methanol as desolvating agent at lower concentrations (60-80 %) led to NPs in a size range of 70-95 nm with higher polydispersity. For methanol at concentrations of 90% the particle size of NPs remained constant at about 70 nm but slightly reduced polydispersity was observed. In case of desolvating agent acetone and ethanol, increasing concentrations led to higher particle size of NPs whereas in case of desolvating agent methanol, increasing concentrations has not affected the particle size of NPs may due higher dielectric constant of methanol (Dielectric constant of methanol: 32.7) and the correlation exist between particle size of NPs and dielectric constant of desolvating agent (Higher dielectric constants led to smaller particles whereas lower dielectric constants led to larger particles). The particles obtained by protein desolvation with ethanol in contrast to acetone, were monodisperse at every solvent concentration and the particle preparations with ethanol and acetone showed an

intense turbidity, indicating a higher yield of NPs. The turbidity of the resulting suspension varied between an intense milky appearance and a slight opalescence. Although the opalescence mainly depends on the light scattering due to particle size of NPs hence turbidity can be taken as a crude estimation for particle yield. In this study for more precise determination of the particle yield, quantification of the undesolvated amount of HSA in the supernatant of the NPs was performed by BSA estimation procedure. Under all preparation conditions, below 0.05 % of undesolvated HSA was detected. Based on the size requirement for i.v. administration ethanol was selected as desolvating agent for further study.

Stirring Rate: HSA NP preparation was carried out with ethanol 70% (m/m) using different stirring rates ranging from 200 to 1000 rpm. By using ethanol and a stirring rate of 200 rpm, the mean particle size was nearly 450 nm and a polydispersity index of 0.43 showed a relative broad particle size distribution. Higher stirring rates up to 500 rpm resulted in smaller particles of around 150 nm and lower polydispersity, whereas the size remained nearly constant at stirring rates above 500 rpm.

Addition system of desolvating agent: In order to prevent a local high solvent concentration during desolvation, a continuous versus discontinuous addition of desolvating agent during the preparation process was compared. A significantly decreased particle size was observed by continuous solvent addition. Although no significant difference was observed in the polydispersity of the resulting NPs, the continuous addition showed an advantage over the discontinuous procedure resulting in smaller particles; results are in good agreement with the considerations about local protein precipitation during discontinuous solvent addition.

5.8.2 Optimization by Central Composite Design

Total 30 batches of VBT-HSA-NPs were prepared as CCD by varying the four independent variables albumin concentration (mg/ml) (X_1), vinorelbine (mg) (X_2) pH (X_3), glutaraldehyde concentration (%) (X_4) and evaluated for particle size in nm (Y_1) and % EE (Y_2). Results of analysis are given in **Table 5.6**.

Table 5. 6 Particle size, zeta potential and % EE results of VBT-HSA-NPs by CCD

Formulation Code	Run	Point Type	Independent Variables				Dependent Variable	
			X_1	X_2	X_3	X_4	Y_1 (nm)	Y_2 (%)
F 1	15	Factorial	10	1.5	7.5	75	451.7	45.56
F 2	5	Factorial	20	1.5	7.5	75	325.8	58.7
F 3	2	Factorial	10	1.5	7.5	75	258.4	77.89
F 4	18	Factorial	20	1.5	7.5	75	252.4	74.67
F 5	22	Factorial	10	1.5	8.5	75	177.6	58.45
F 6	8	Factorial	20	1.5	8.5	75	203.9	52.54
F 7	6	Factorial	10	1.5	8.5	75	295.8	68.24
F 8	27	Factorial	20	1.5	8.5	75	252.8	80.41
F 9	1	Factorial	10	2.5	7.5	125	346.7	60.58
F 10	7	Factorial	20	1.5	7.5	125	336.8	74.68
F 11	20	Factorial	10	0.5	7.5	125	341.8	76.53
F 12	3	Factorial	20	1.5	7.5	125	404.8	73.95
F 13	26	Factorial	10	1.5	8.5	125	177.9	76.52
F 14	9	Factorial	20	1.5	8.5	125	182.8	79.14
F 15	10	Factorial	10	1.0	8.5	125	375.9	78.54
F 16	17	Factorial	20	2.0	8.5	125	375.8	82.81
F 17	12	Axial	5	2.0	8.0	100	452.3	68.23
F 18	29	Axial	25	1.0	8.0	100	399.6	78.98
F 19	24	Axial	15	2.0	8.0	100	134.9	53.56
F 20	13	Axial	15	1.0	8.0	100	185.9	73.78
F 21	11	Axial	15	1.0	7.0	100	521.8	66.56
F 22	25	Axial	15	1.0	9.0	100	228.7	67.46
F 23	30	Axial	15	2.0	8.0	50	211.9	77.19
F 24	21	Axial	15	1.0	8.0	150	290.7	73.23
F 25	19	Center	15	2.0	8.0	100	334.6	73.98
F 26	28	Center	15	2.0	8.0	100	311.7	68.98
F 27	14	Center	15	2.0	8.0	100	368.6	71.98
F 28	16	Center	15	1.0	8.0	100	327.5	75.78
F 29	4	Center	15	1.0	8.0	100	316.4	76.89
F 30	23	Center	15	2.0	8.0	100	361.3	79.54

On the basis of the results obtained in the preliminary screening studies, the high and low levels of albumin in mg/ml (X_1), vinorelbine amount in mg/ml (X_2), pH (X_3) and % glutaraldehyde concentration (X_4) were selected for further study. In order to investigate the factors systematically, a CCD was employed for optimization of albumin NPs. The particle size and % EE for the 30 batches (F1 to F30) showed a wide variation 134.9-521.8 nm and 45.56 - 82.81 % respectively given **Table 5.6**. Optimization results of analysis for particle size and % EE clearly indicate that the results of response variables are strongly dependent on the selected independent variables. Optimization results of analysis for particle size (nm) and entrapment efficiency (%) are given below.

5.8.2.1 Statistical Analysis of Particle Size (Response 1)

Sequential p-value, lack of fit p-value, adjusted R^2, predicted R^2 values and suggested model are given in the **Table 5.7**.

Table 5. 7 Summary of ANOVA results (Particle Size) for Different Models

Source	Sequential p-value	Lack of Fit p-value	Adjusted R-Squared	Predicted R-Squared	Model Suggested
Linear	0.0302	0.0034	0.2320	-0.0190	----
2FI	0.1727	0.0044	0.3440	0.1731	----
Quadratic	< 0.0001	0.1626	0.8755	0.6755	Suggested
Cubic	0.0814	0.4775	0.9401	0.4515	Aliased*

*The Cubic Model and higher are aliased. This shows that the predicted responses would be confounded by the other factors implying that the predicted response would give the wrong idea of the actual response.

Table 5.7 suggested the best model to fit the experimental results of particle size of NPs is quadratic model and results of ANOVA analysis of the suggested quadratic model given in **Table 5.8**.

Table 5. 8 ANOVA for Response Surface Quadratic Model (Particle Size)

Source	Sum of Squares	df	Mean Square	F Value	p-value Prob > F	
Model	2.390E+005	14	17072.61	15.56	< 0.0001	**Significant**
X_1-Albumin Conc.	1602.30	1	1602.30	1.46	0.2455	
X_2-VBT Amount	8683.01	1	8683.01	7.92	0.0131	
X_3-pH	66370.68	1	66370.6	60.51	< 0.0001	
X_4-Glu. Conc.	9668.12	1	9668.12	8.81	0.0096	
X_1X_2	877.64	1	877.64	0.80	0.3852	
X_1X_3	279.73	1	279.7	0.26	0.6209	
X_1X_4	2665.14	1	2665.14	2.43	0.1399	
X_2X_3	36261.68	1	36261.68	33.06	< 0.0001	
X_2X_4	19161.48	1	19161.48	17.47	0.0008	
X_3X_4	102.52	1	102.52	0.093	0.7640	
X_1^2	12528.19	1	12528.19	11.42	0.0041	
X_2^2	55581.44	1	55581.44	50.67	< 0.0001	
X_3^2	2074.58	1	2074.58	1.89	0.1892	
X_4^2	13628.49	1	13628.49	12.42	0.0031	
Residual	16453.52	15	1096.90			
Lack of Fit	13704.62	10	1370.46	2.49	0.1626	**Not**
Pure Error	2748.91	5	549.78			**significant**
Cor Total	2.555E+005	29				
Std. Dev.	33.12		**R-Squared**	0.9356		
Mean	306.89		**Adj R-Squared**	0.8755		
C.V. %	10.79		**Pred R-Squared**	0.6755		
PRESS	82897.02		**Adeq Precision**	15.290		

The Model F-value of 15.56 implies the model is significant. There is only a 0.01% chance that a "Model F-Value" this large could occur due to noise. Values of "Prob > F" less than 0.0500 indicate model terms are significant. In this case vinorelbine amount, pH, glutaraldehyde concentration, interaction between vinorelbine amount & pH and vinorelbine amount & glutaraldehyde concentration as well as

quadtratic effect of albumin concentration, vinorelbine amount and glutaraldehyde concentration are the significant model terms. Values greater than 0.1000 indicate the model terms are not significant. The "Lack of Fit F-value" of 2.49 implies the Lack of Fit is not significant relative to the pure error. There is a 16.26% chance that a "Lack of Fit F-value" this large could occur due to noise. Non-significant lack of fit is good in our studies because we want the model to fit. The "Pred R-Squared" of 0.6755 is in reasonable agreement with the "Adj R-Squared" of 0.8755. "Adeq Precision" measures the signal to noise ratio. A ratio greater than 4 is desirable. Our ratio of 15.290 indicates an adequate signal.

Final Polynomial Equation in Terms of Coded Factors for Particle Size

$$= +336.68$$
$$-8.17*X_1 +19.02 * X_2 -52.59 * X_3 +20.07 * X_4$$
$$+7.41*X_1* X_2 +4.18* X_1* X_3 +12.91* X_1 * X_4$$
$$+47.61 * X_2 * X_3 +34.61 * X_2 * X_4 +2.53*X_3*X_4$$
$$+21.37 * X_1^2 -45.02 * X_2^2 +8.70 * X_3^2 -22.29 * X_4^2$$

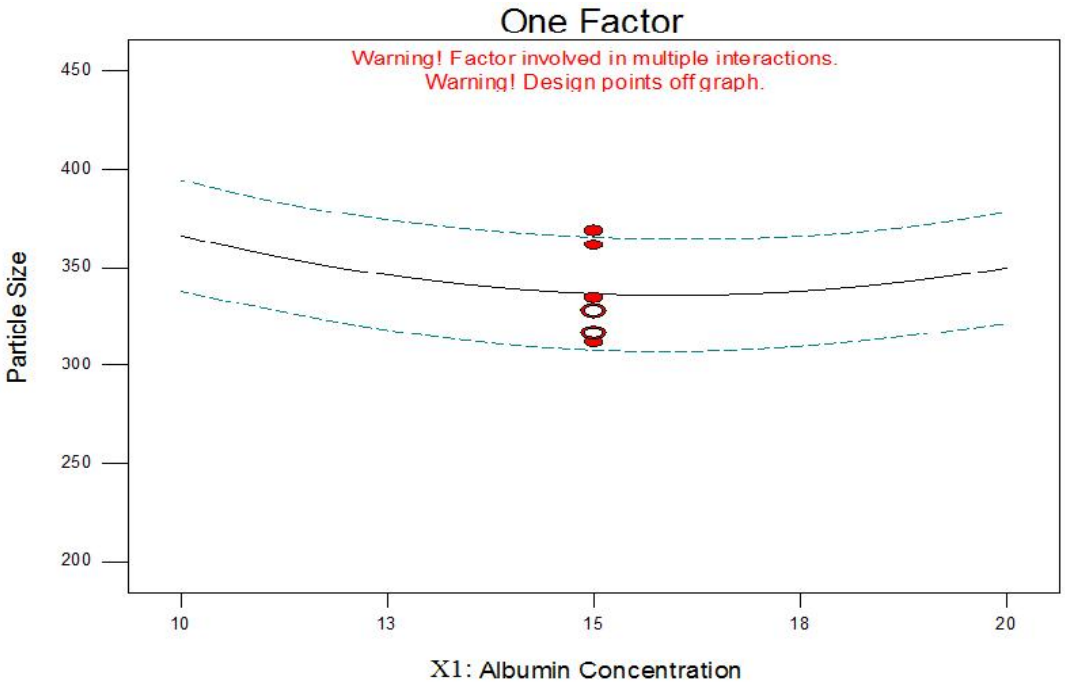

Figure 5. 2 Effect of Albumin Concentration on Particle Size

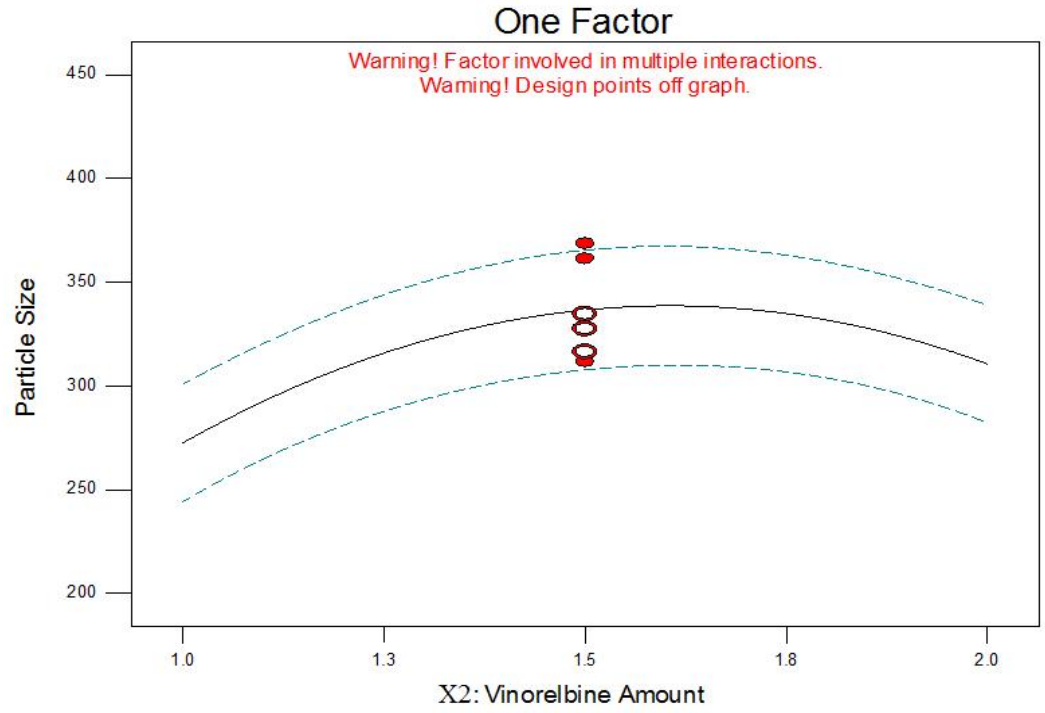

Figure 5. 3 Effect of Vinorelbine Amount on Particle Size

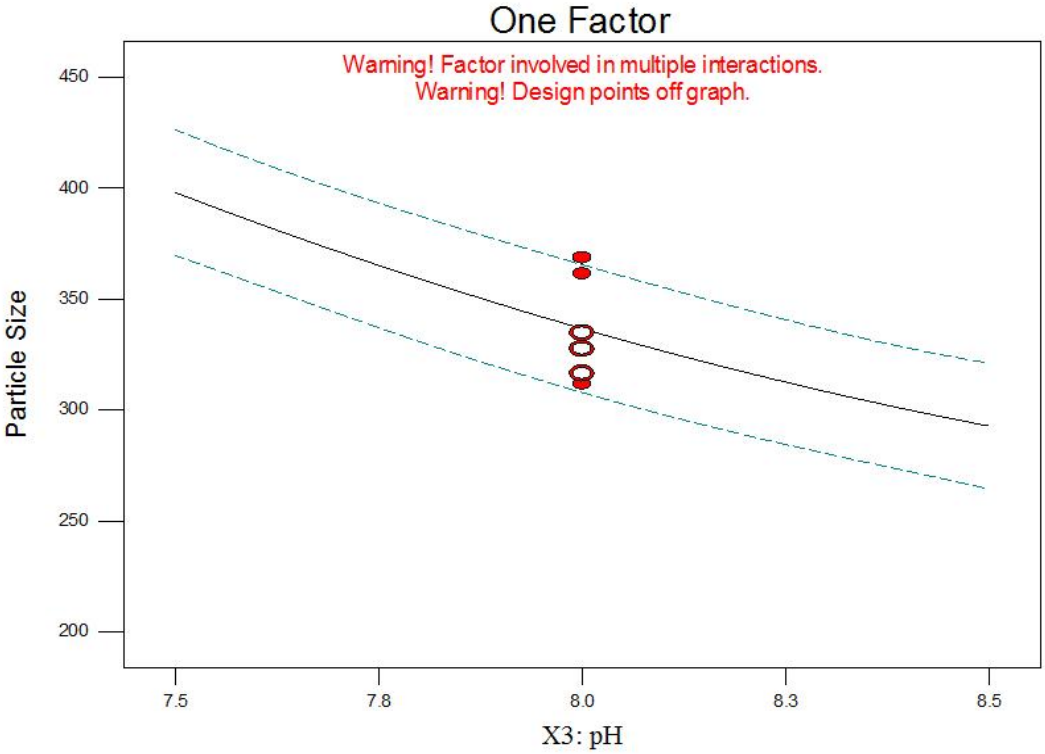

Figure 5. 4 Effect of pH on Particle Size

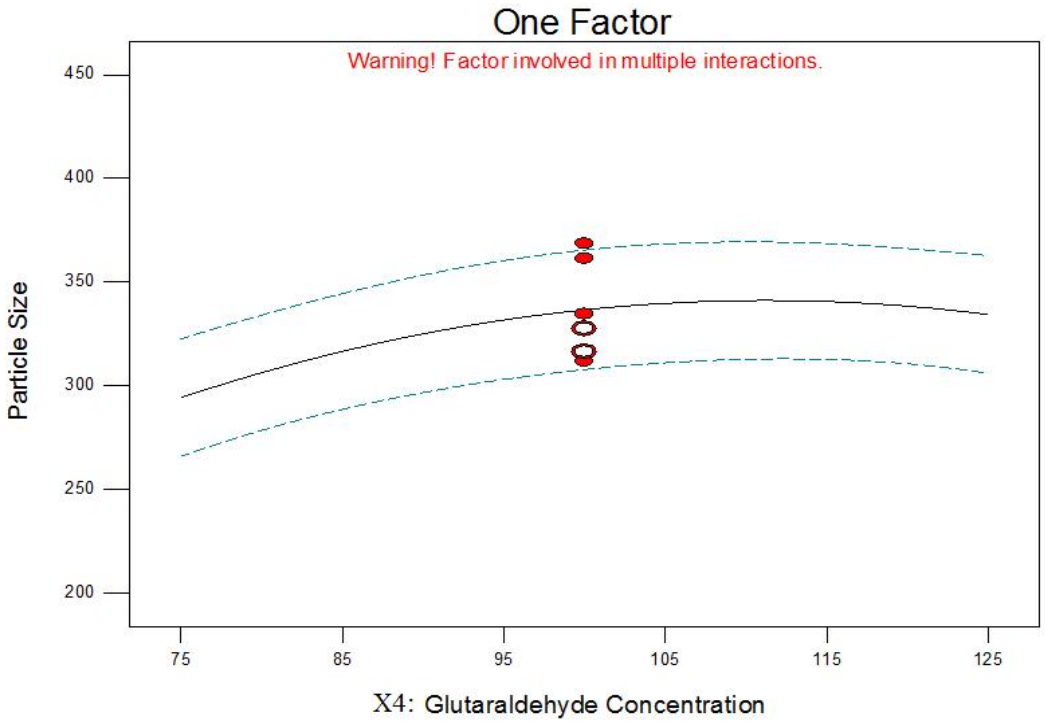

Figure 5. 5 Effect of Glutardaldyde Concentration on Particle Size

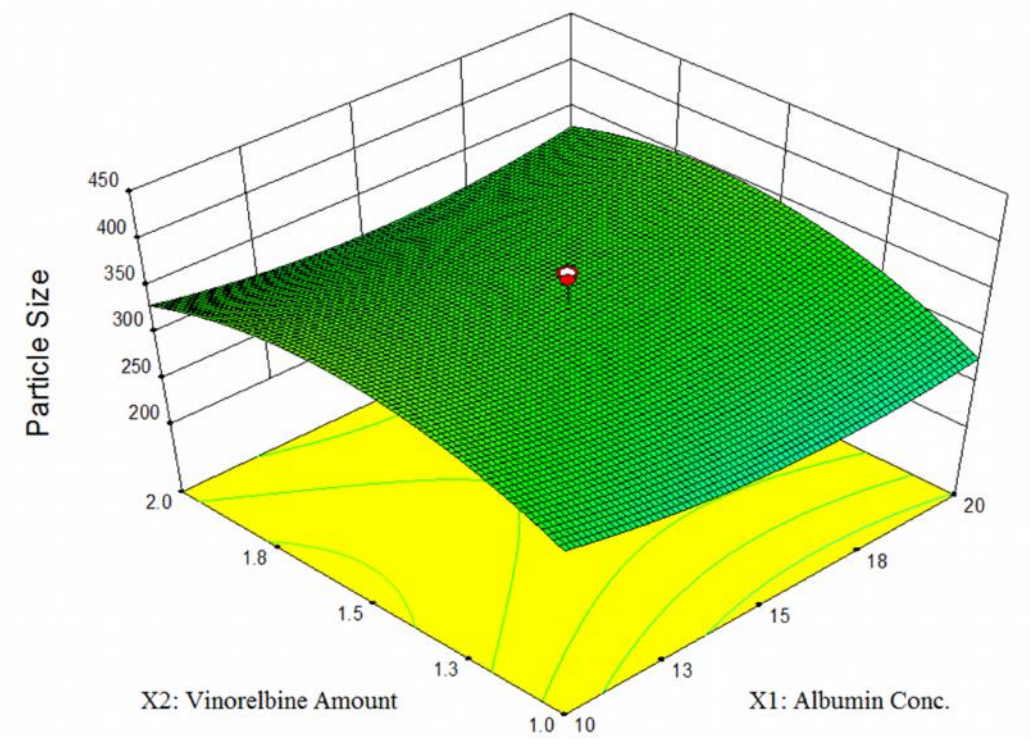

Figure 5. 6 Response Surface Showing Combined Effect of Vinorelbine Amount and Albumin Concentration on Particle Size

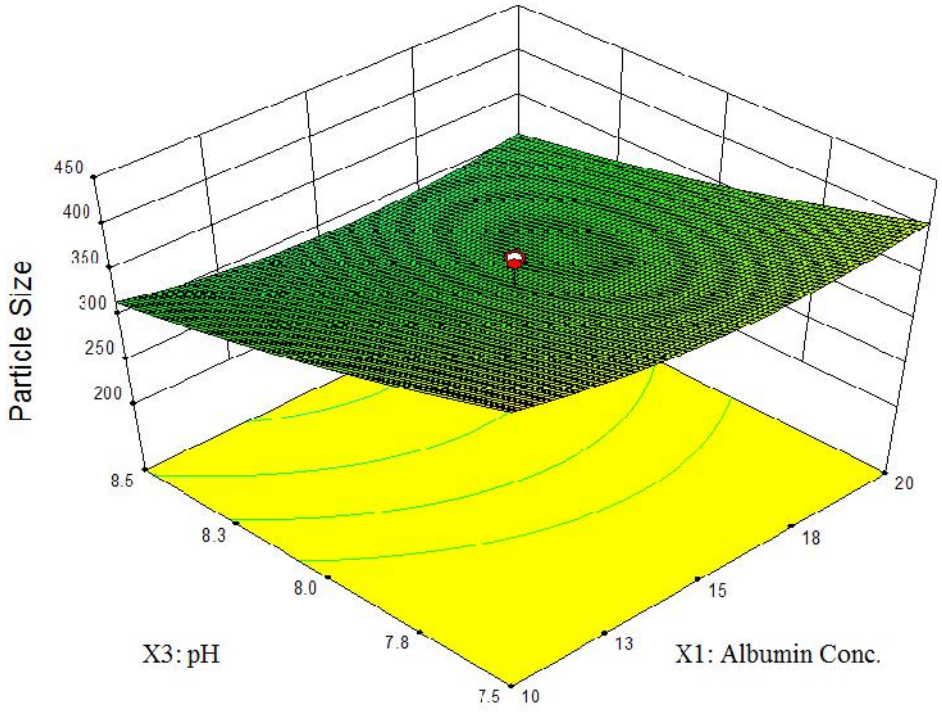

Figure 5. 7 Response Surface Showing Combined Effect of pH and Albumin Concentration on Particle Size

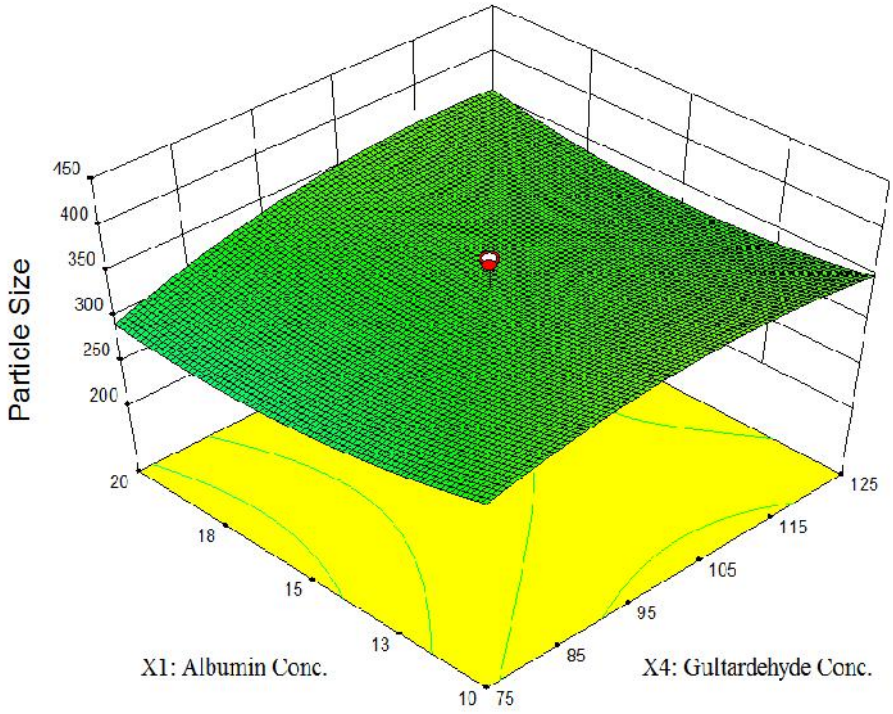

Figure 5. 8 Response Surface Showing Combined Effect of Glutardaldyde Concentration and Albumin Concentration on Particle Size

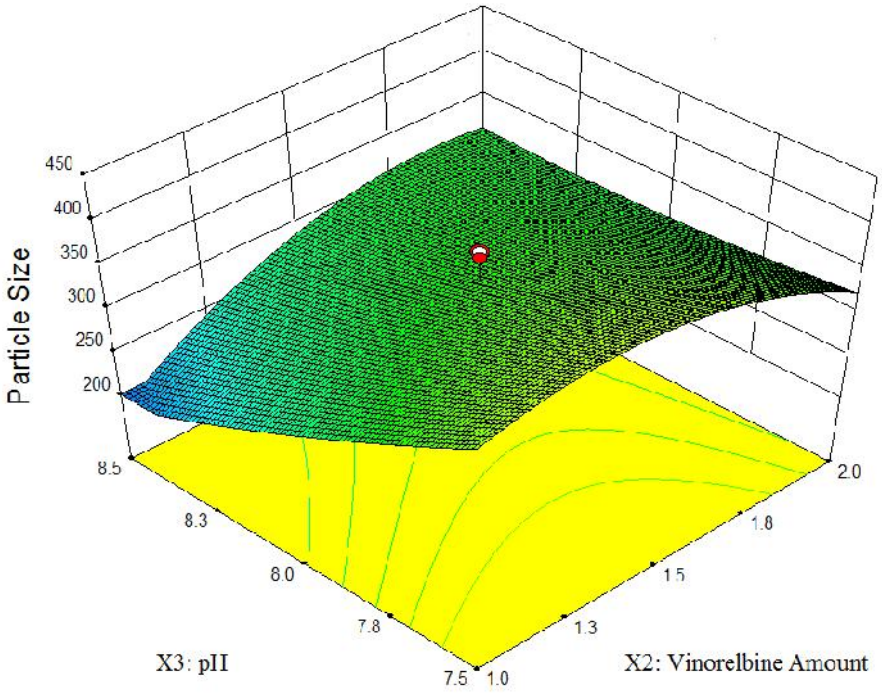

Figure 5. 9 Response Surface Showing Combined Effect of Vinorelbine Amount and pH on Particle Size

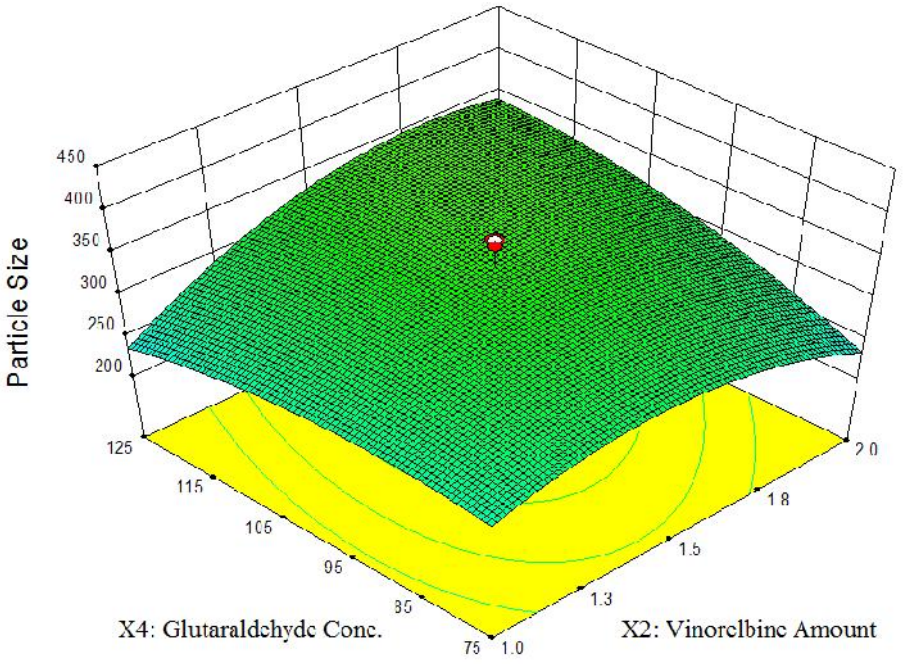

Figure 5. 10 Response Surface Showing Combined Effect of Vinorelbine Amount and Glutardaldyde Concentration on Particle Size

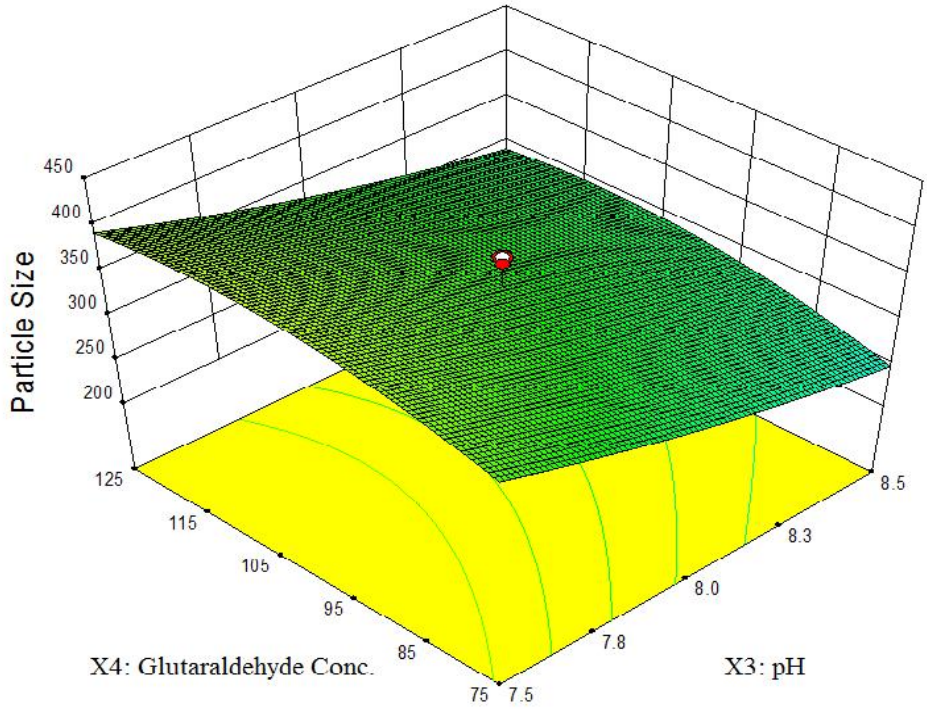

Figure 5. 11 Response Surface Showing Combined Effect of pH and Glutardaldyde Concentration on Particle Size

From response surface plots it was found that both drug concentration and albumin concentration had quadratic effect on particle size of NPs but trend of both factors on response was opposite i.e. increase in albumin concentration leads to reduction in particles size which attains a minimum and again rise on further increase of albumin concentration while when drug concentration is increased particles size increases and later on decreases after attaining maximum size. There was continuous reduction in size with increase in pH. When effect of glutaraldehyde concentration on particle size was checked it was found that on increasing its concentration there was increase in particle size which attains maximum and then there was no further increase in size after that point.

5.8.2.2 Statistical Analysis of % EE (Response 2)

Sequential p-value, lack of fit p-value, adjusted R^2, predicted R^2 values and suggested model are given in the **Table 5.9**.

Table 5. 9 Summary of ANOVA results (% EE) for Different Models

Source	Sequential p-value	Lack of Fit p-value	Adjusted R-Squared	Predicted R-Squared	Model Suggested
Linear	0.0005	0.0677	0.4613	0.3041	Suggested
2FI	0.2681	0.0748	0.5077	0.0433	
Quadratic	0.1495	0.1002	0.5919	0.0958	
Cubic	0.0310	0.5927	0.8579	0.0278	Aliased*

*The Cubic Model and higher are aliased. This shows that the predicted responses would be confounded by the other factors implying that the predicted response would give the wrong idea of the actual response.

Table 5.9 suggested the best model to fit the experimental results of %EE of NPs is quadratic model and results of ANOVA analysis of the suggested model given in **Table 5.10**.

Table 5. 10 ANOVA for Response Surface Model (% EE)

Source	Sum of Squares	df	Mean Square	F Value	p-value Prob > F	
Model	1980.75	14	141.48	4.00	0.0058	**significant**
X_1-Albumin Conc.	131.09	1	131.09	3.71	0.0733	
X_2-VBT Amount	904.18	1	904.18	25.59	0.0001	
X_3-pH	53.67	1	53.67	1.52	0.2368	
X_4-Glu. Conc.	255.91	1	255.91	7.24	0.0168	
X_1X_2	11.07	1	11.07	0.31	0.5839	
X_1X_3	4.30	1	4.30	0.12	0.7322	
X_1X_4	0.31	1	0.31	8.796	0.9265	
X_2X_3	25.43	1	25.43	E-003	0.4096	
X_2X_4	264.47	1	264.47	0.72	0.0153	
X_3X_4	50.59	1	50.59	7.48	0.2501	
X_1^2	1.29	1	1.29	1.43	0.8508	
X_2^2	200.09	1	200.09	0.037	0.0310	
X_3^2	95.50	1	95.50	5.66	0.1210	
X_4^2	0.93	1	0.93	2.70	0.8733	

Residual	530.02	15	35.33	0.026		
Lack of Fit	460.18	10	46.02		0.1002	**Not**
Pure Error	69.84	5	13.97	3.29		**significant**
Cor Total	2510.77	29				
Std. Dev.	5.94		**R-Squared**		0.7889	
Mean	70.85		**Adj R-Squared**		0.5919	
C.V. %	8.39		**Pred R-Squared**		-0.0958	
PRESS	2751.22		**Adeq Precision**		7.220	

The Model F-value of 4.00 implies the model is significant. There is only a 0.58% chance that a "Model F-Value" this large could occur due to noise. Values of "Prob > F" less than 0.0500 indicate model terms are significant. In this case vinorelbine amount , glutaraldehyde conc., interataction beween vinorelbine amount & glutaraldehyde conc. and qudratic effect of vinorelbine amount are significant model terms. Values greater than 0.1000 indicate the model terms are not significant. The "Lack of Fit F-value" of 3.29 implies the Lack of Fit is not significant relative to the pure error. There is a 10.02% chance that a "Lack of Fit F-value" this large could occur due to noise. Non-significant lack of fit is good our studies indicate that the model is fit. A negative "Pred R-Squared" implies that the overall mean is a better predictor of your response than the current model. "Adeq Precision" measures the signal to noise ratio. A ratio greater than 4 is desirable. Your ratio of 7.220 indicates an adequate signal.

Final Polynomial Equation in Terms of Coded Factors for Encapsulation Efficiency

$$= +74.53 + 2.34 * X_1 + 6.14 * X_2 + 1.50 * X_3 + 3.27 * X_4$$
$$-0.83 * X_1 * X_2 - 0.52 * X_1 * X_3 + 0.14 * X_1 * X_4$$
$$-1.26 * X_2 * X_3 - 4.07 * X_2 * X_4 + 1.78 * X_3 * X_4$$
$$-0.22 * X_1^2 - 2.70 * X_2^2 - 1.87 * X_3^2 + 0.18 * X_4^2$$

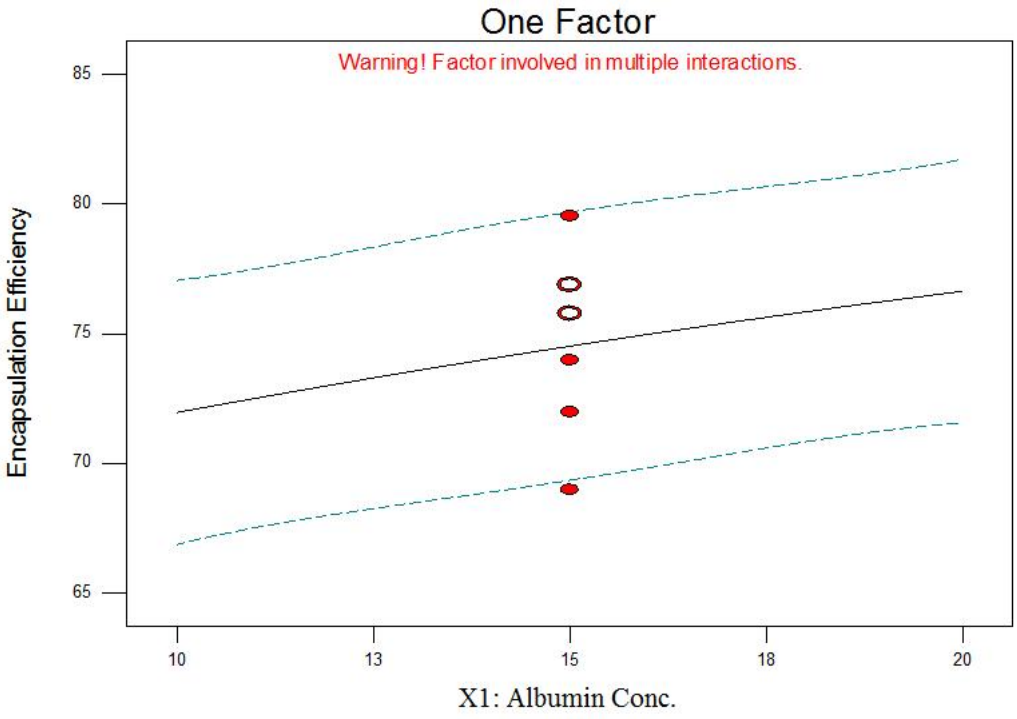

Figure 5. 12 Effect of Albumin Concentration on Encapsulation Efficiency

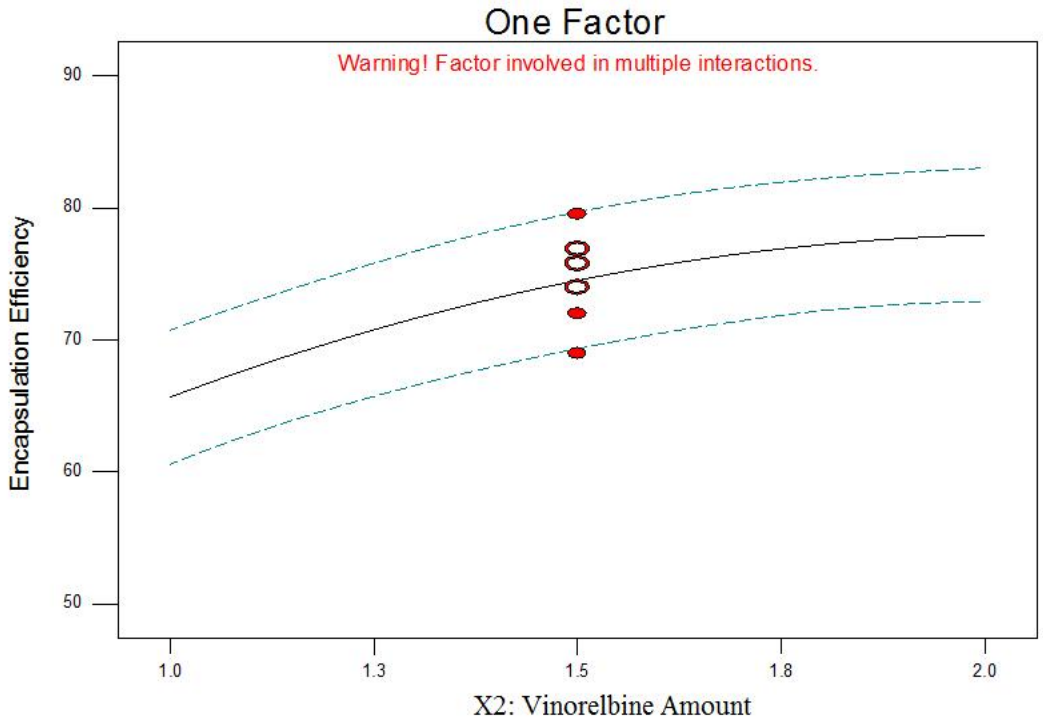

Figure 5. 13 Effect of Vinorelbine Amount on Encapsulation Efficiency

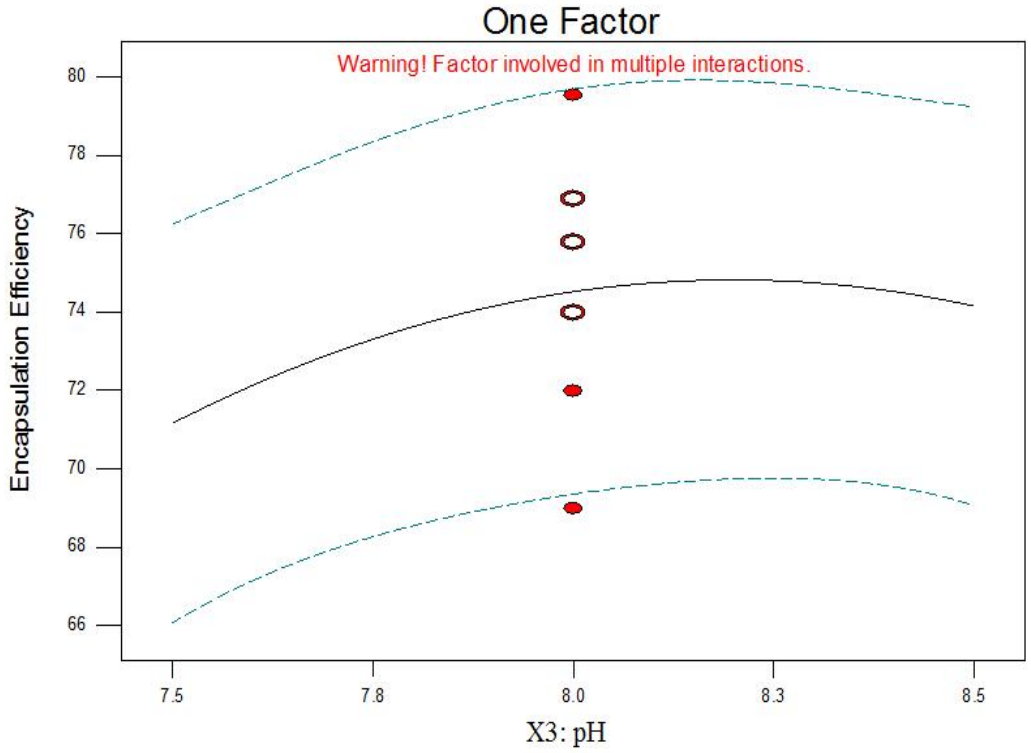

Figure 5. 14 Effect of pH on Encapsulation Efficiency

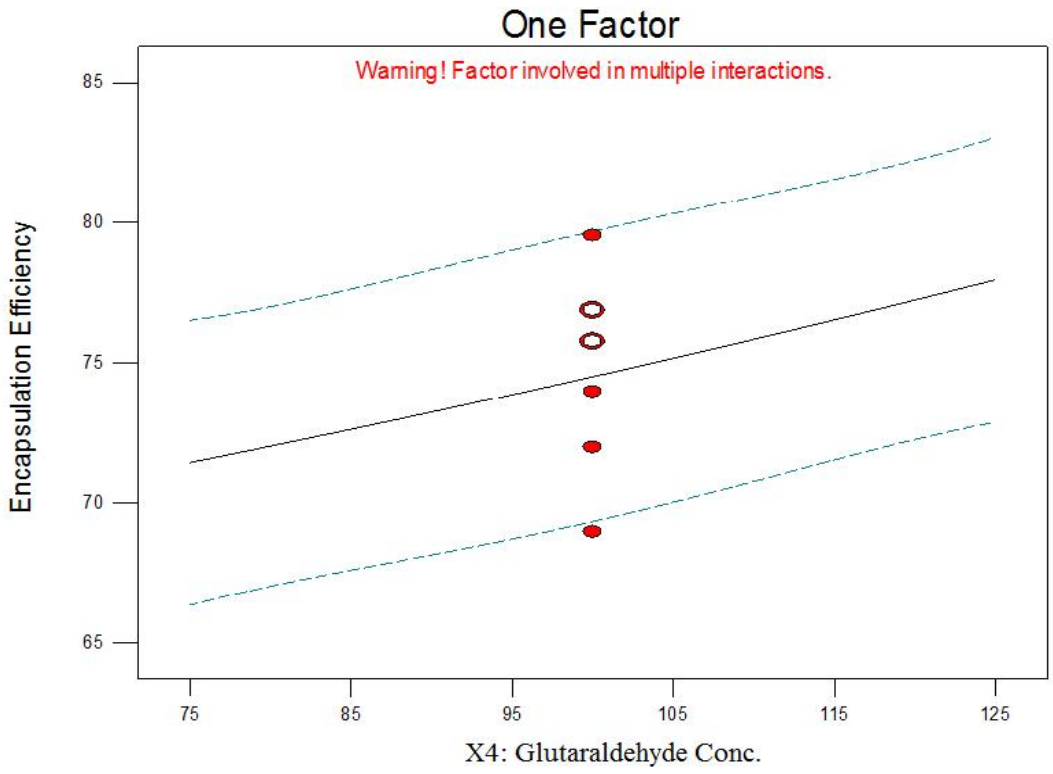

Figure 5. 15 Effect of Glutaraldehyde Concentration on Encapsulation Efficiency

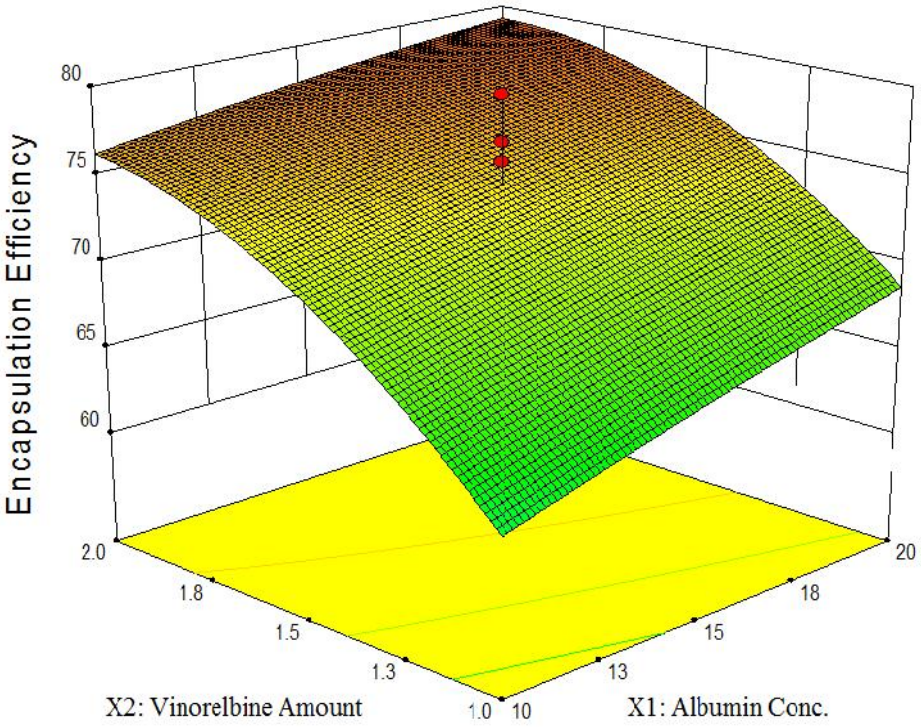

Figure 5. 16 Response Surface Showing Combined Effect of Vinorelbine Amount and Albumin Concentration on Encapsulation Efficiency

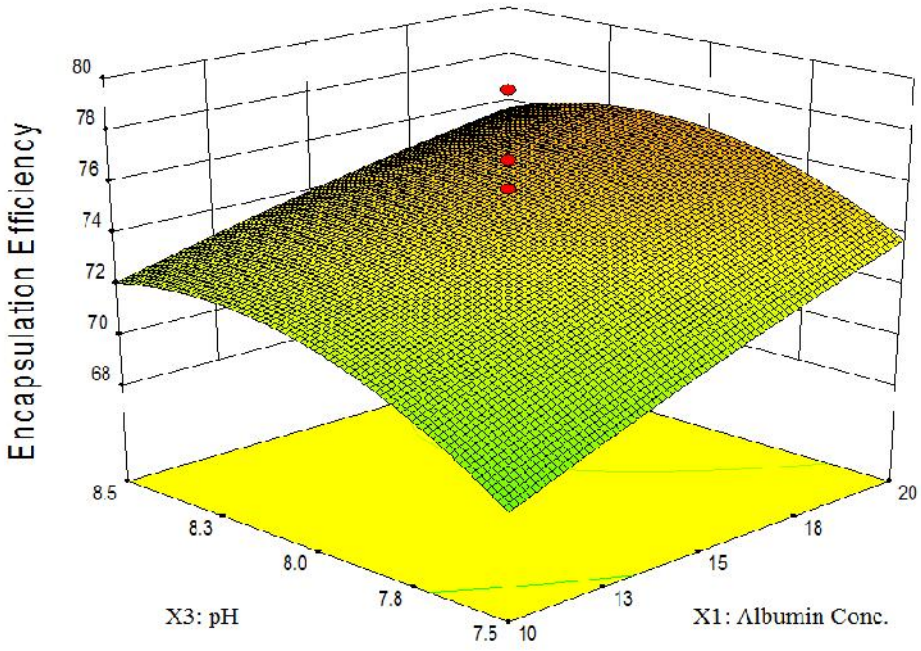

Figure 5. 17 Response Surface Showing Combined Effect of pH and Albumin Concentration on Encapsulation Efficiency

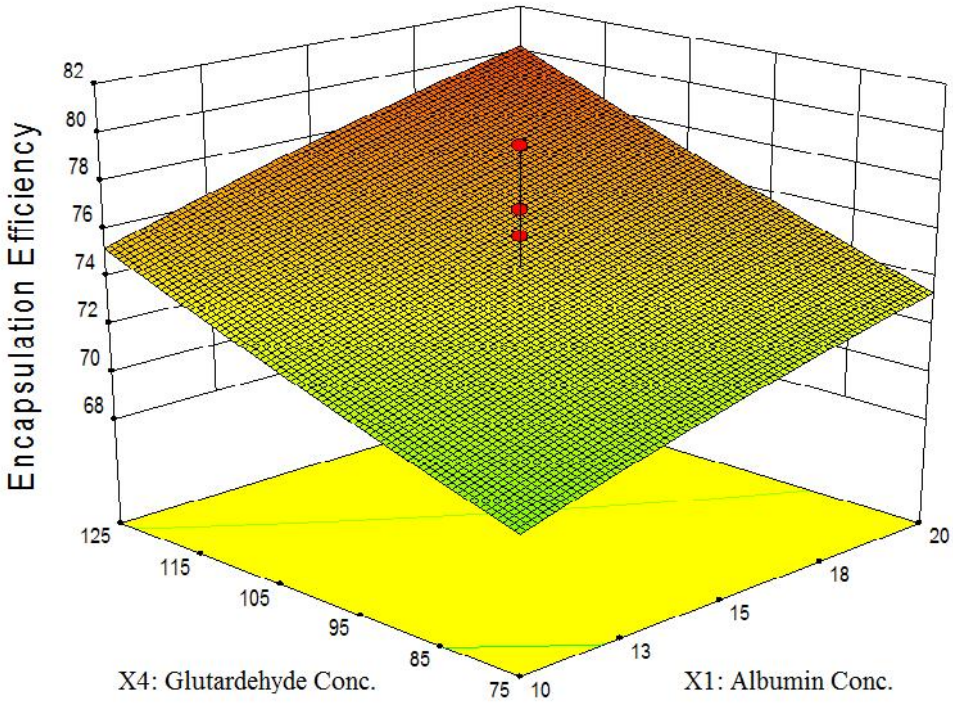

Figure 5. 18 Response Surface Showing Combined Effect of Albumin Concentration and Glutardaldyde Concentration on Encapsulation Efficiency

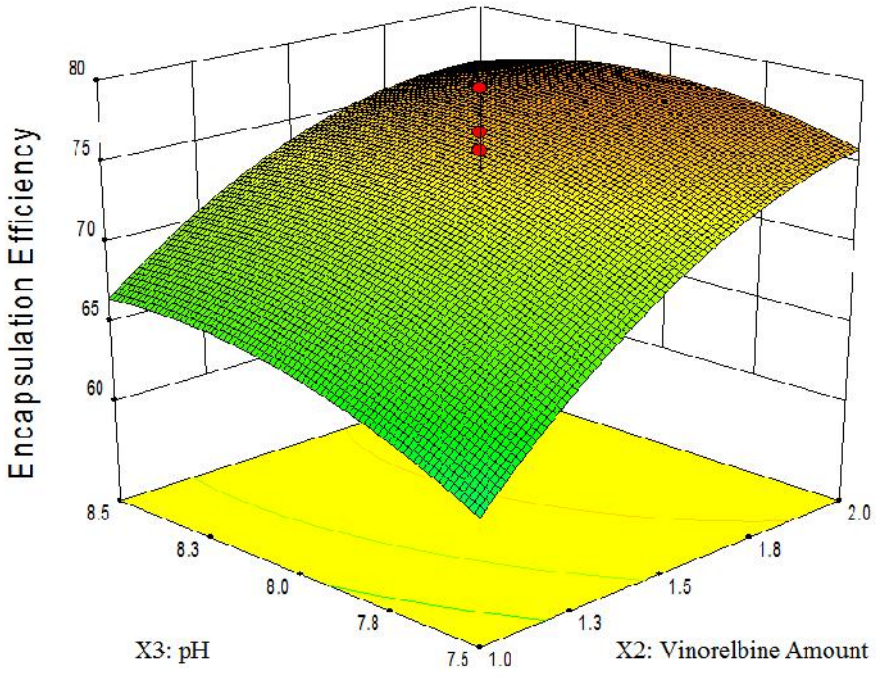

Figure 5. 19 Response Surface Showing Combined Effect of pH and Vinorelbine Amount on Encapsulation Efficiency

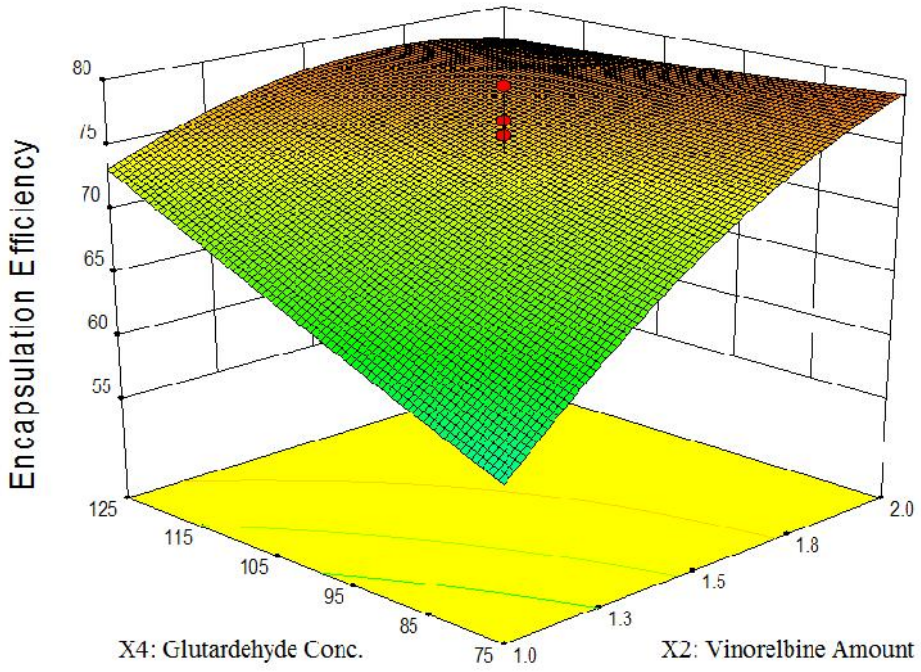

Figure 5. 20 Response Surface Showing Combined Effect of pH and Glutardaldyde Concentration on Encapsulation Efficiency

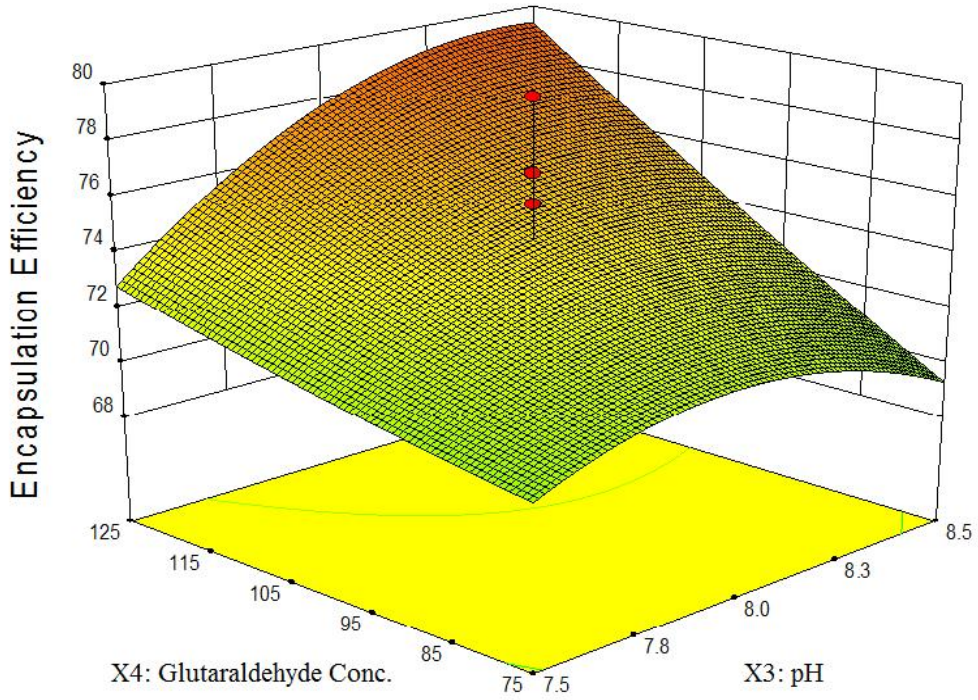

Figure 5. 21 Response Surface Showing Combined Effect of pH and Glutardaldyde Concentration on Encapsulation Efficiency

From response surface plots it was found that drug concentration, albumin concentration and glutaraldehyde concentration had relatively similar effect on entrapment efficiency i.e. on increasing concentration there was continuous improvement of entrapment efficiency. But effect of pH on entrapment efficiency on entrapment efficiency was found quadratic i.e. the entrapment efficiency increases with increase in pH till it attains maximum and later on there was slight decrease in entrapment efficiency on further rise of pH.

The equation can be used to obtain estimates of the responses. Factor X_1 (amount of albumin) has a negative effect on particle size indicated by the negative signs of coefficient X_1 (-8.17) whereas positive effect entrapment efficiency indicated by the positive signs of coefficient X_1 (+2.34). Factor X_2 (amount of drug) shows positive effect on particle size as well as on entrapment efficiency indicated by the positive sign of coefficient X_2 (+19.02 and +6.14 respectively). Factor X_3 (pH) shows negative effect on particle size indicated by the negative signs of coefficient X_3 (-52.59) whereas positive effect on particle size and entrapment efficiency as shown by the positive sign of coefficient X_3 (+1.50). Factor X_4 (% Glutaraldehyde) shows positive effect on particle size as well as on entrapment efficiency indicated by the positive sign of coefficient X_4 (+20.07 and +3.27). Similarly, effects of different interaction terms such as X_1X_2, X_1X_3, X_1X_4, X_2X_3, X_2X_4 and X_3X_4 on response variables can be seen from the signs and values of X_1X_2, X_1X_3, X_1X_4, X_2X_3, X_2X_4 and X_3X_4 respectively. X_1^2, X_2^2, X_3^2 and X_4^2 terms are second order terms and are useful to estimate non linearity of response.

As can be seen from **Figure 5.4** the particle size (Y_1) decreased markedly with the increase of pH. With increasing pH values the zeta potential of the NPs was also reduced. When the albumin concentration and amount of VBT were held at center point, namely 15 mg/ml and 1.5 mg/ml, the zeta potential of the NPs have a maximal value as the pH and percentage of glutaraldehyde arrive at 8.5 and 100%, respectively. In the case of encapsulation efficiency (Y_2), as the amount of VBT and % of glutaraldehyde increased, the % EE also increased. When the albumin concentration and pH were held at center point, namely 15 mg/ml and 8.0, encapsulation efficiency of the NPs has a maximal value 79.54 % as the amount of VBT and % of glutaraldehyde arrive at 1.5 mg/ml and 100%, respectively.

After the polynomial equations have been generated, the formulation was optimized for the responses Y_1 (mean particle size (nm)) and Y_2 (% EE). The optimum

values of the variables were obtained by graphical and numerical analyses using the Design- Expert® software and based on the criterion of desirability. Afterwards, a new batch of NPs with the predicted levels of formulation factors was prepared to confirm the validity of the optimization procedure. **Table 5.12** demonstrates that the observed values of a new batch were mostly similar with predicted values within ±2.293 % of predicted error. The optimized formulation was achieved with 17 mg/ml albumin, 1 mg/ml VBT, pH value is 8.5 and 125% percentage of glutaraldehyde conc. Thus, five new batches of the VBT-HSA-NPs were prepared to confirm the validity of the optimization procedure. **Table 5.12** indicates a predicted error of 1.975 % for mean particle size and -2.293 % for encapsulation efficiency (%). Hereafter, all of the experiments will be conducted using VBT-HSA-NPs produced by this optimized formulation. Composition of optimized batches and comparison of the observed responses with that of the predicted responses along with percentage error given **Table 5.12**. Desirability plots for optimized formulation is shown in **Figure 5.22**.

The polynomial equations form excellent fit to the experimental data and are highly statistically valid. The criteria for selection of suitable feasible region (from the intensive grid search) were primarily based on minimum particle size and the highest possible values of % EE.

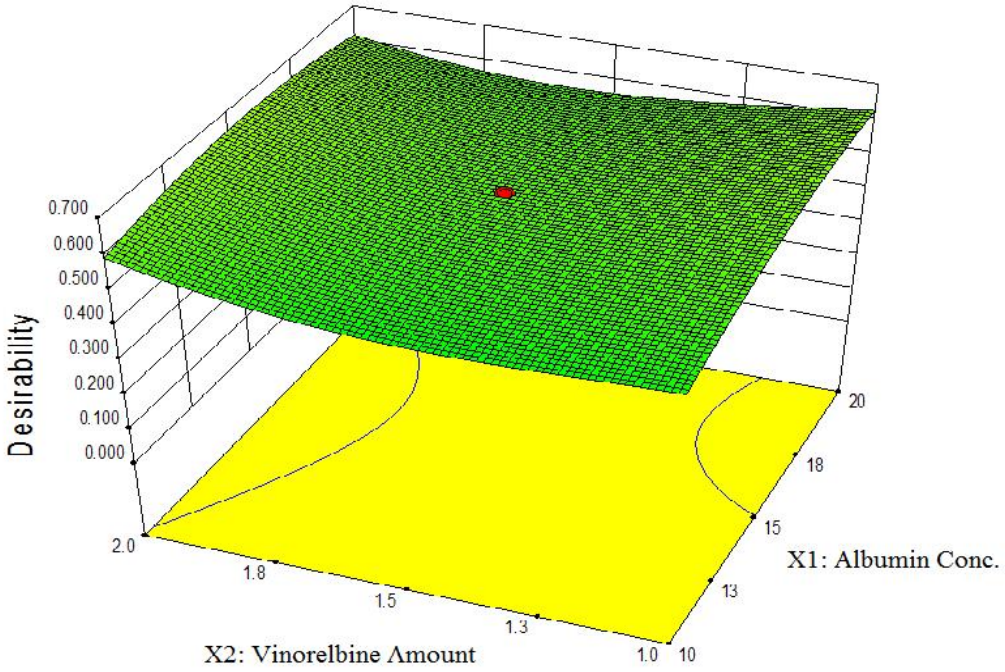

Figure 5. 22 Desirability Plot for Optimized Formulations

Table 5. 11 Comparison of observed responses of optimized formulation with predicted responses.

Optimized Formulation Composition	Response	Predicted value	SD	SE	95% CI low	95% CI high	Observed value	Percent error
Albumin (17 mg/ml) Drug (1 mg/ml) pH (8.5) Glutaraldehyde Conc. (125%)	Particle Size	151.311	33.119	21.009	106.531	196.091	154.3	1.975
	% EE	77.006	5.944	3.770	68.969	85.043	75.24	-2.293

5.8.3 Characterization

5.8.3.1 Particle sizes, zeta potential and encapsulation efficiency

The particle size and zeta potential of optimized formulation were measured in triplicates and the results were 154.3±4.72 nm and -15.6±2.074 mV respectively. The % EE of VBT-HSA-NPs was found 75.24± 2.23% as calculated by following equation.

% EE = (Weight of drug in NPs/ Weight of total drug) ×100

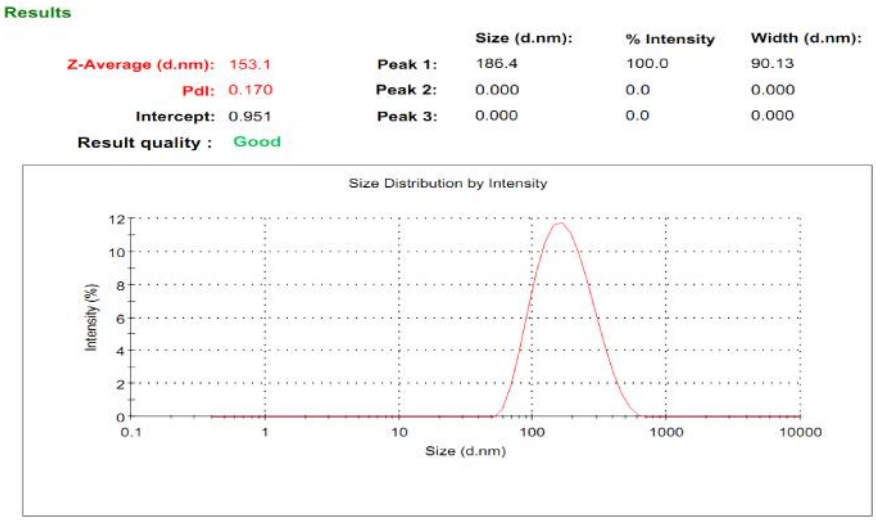

Figure 5. 23 Particle size distributions of optimized VBT HAS NPs by Malvern Zetasizer

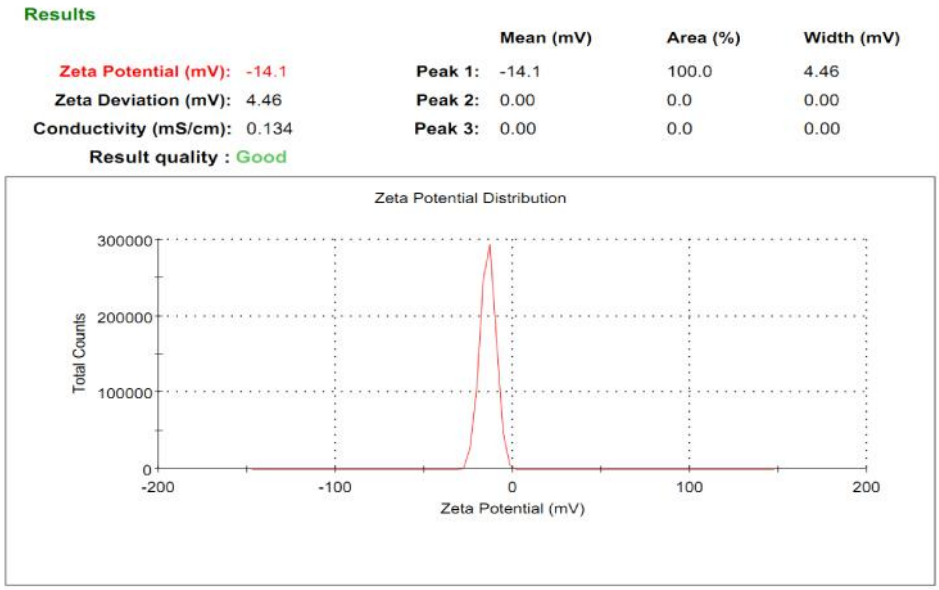

Figure 5. 24 Zeta Potential of optimized VBT HSA NPs by Malvern Zetasizer

5.8.3.2 Transmission Electron Microscopy (TEM)

The surface morphology of the formulated NPs was visualized by TEM. TEM imaging of VBT-HSA-NPs exhibit a spherical shape of NPs as shown in **Figure 5.25.**

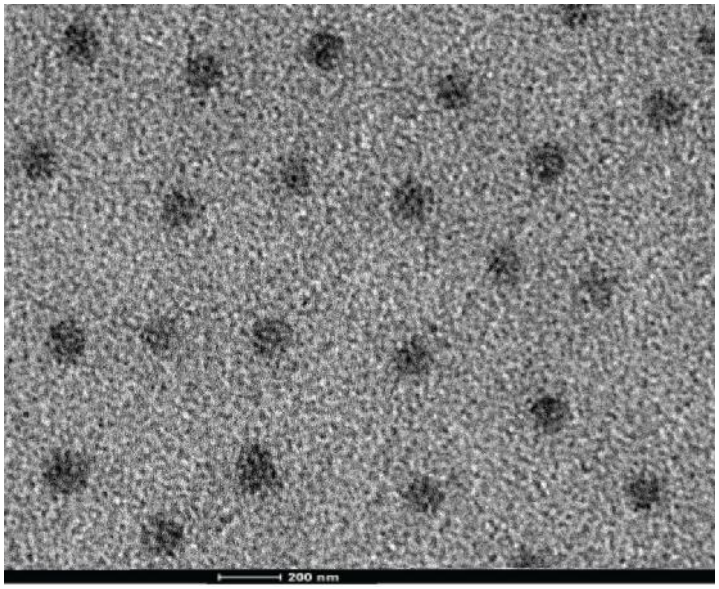

Figure 5. 25 TEM images of VBT-HSA-NPs

5.8.3.3 Differential scanning calorimetry (DSC)

The DSC curves of vinorelbine and human serum albumin showed a melting endotherm at 225º C **(Figure 5.26 A)** and at 70º C **(Figure 5.26 B)** respectively. The raw VBT did not exhibit an obvious melting process, which implied the noncrystalline

form of VBT. In DSC thermogram of physical mixture (VBT and HSA) **(Figure 5.26 C)** a melting endotherm for VBT and HSA were observed and there was no shifting of melting endotherm compared to melting endotherm of single component which indicates compatibility among all components in formulation while no melting process was observed for VBT HSA NPs indicates that NPs were nanostructured and non-crystalline **(Figure 5.26 D)**.

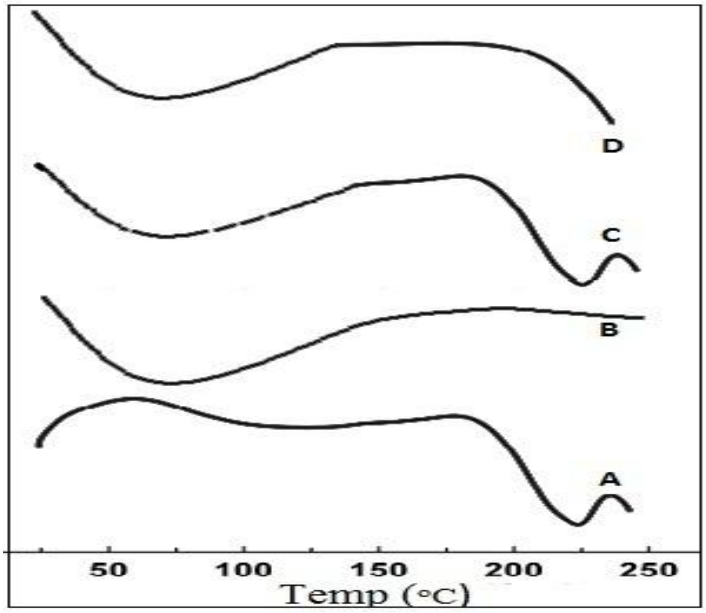

Figure 5. 26 DSC thermogram of vinorelbine (A), Human serum albumin, (B) Physical mixture of vinorelbine and human serum albumin (C) and VBT HSA NPs (D).

5.8.3.4 In vitro drug release

The *in vitro* drug release studies of VBT-HSA-NPs were carried out in trypsin phosphate buffered saline (pH 7.4) by diffusion method for 60 hr and the results were compared by different kinetic models. An initial burst of more than 60% of the plain VBT in first 6 hr was observed then a slow release up to 24 hr. A cumulative release reached 96% for plain VBT, while VBT-HSA-NPs showed a slow release of drug up to 60 hr, releasing approximately 86% of VBT. It is evident that the sustained release of drug from VBT-HSA-NPs will provide a better therapeutic efficacy than plain VBT. After application of different drug release kinetics models, it was observed that the VBT-HSA-NPs followed the Korsmeyer Peppas model because R^2 value (0.9379) which was nearer to 1 and having n value of 0.3798 indicating that drug transport mechanism is Fickian diffusion. *In vitro* drug release data for plain VBT solution and VBT-HSA-NPs given in **Table 5.10** and Drug release pattern shown in **Figure 5.27**.

Table 5. 12 *In vitro* drug release data for plain VBT and VBT-HSA-NPs

Time (h)	Cumulative% Drug Release (Mean ± SD)*	
	Plain drug dispersion	VBT-HSA-NPs
0.5	15.9±0.155	10.81±0.467
1	28.34±0.765	18.86±0.678
2	41.72±1.123	28.32±0.867
4	51.73±1.514	36.68±1.423
6	60.78±1.432	45.56±1.564
8	76.81±1.321	49.75±1.478
12	88.42±1.563	54.21±1.375
24	96.34±1.234	59.31±1.256
36	-	63.45±1.365
48	-	75.65±1.283
60	-	86.25±1.267

* The experiment was performed in triplicate (n=3)

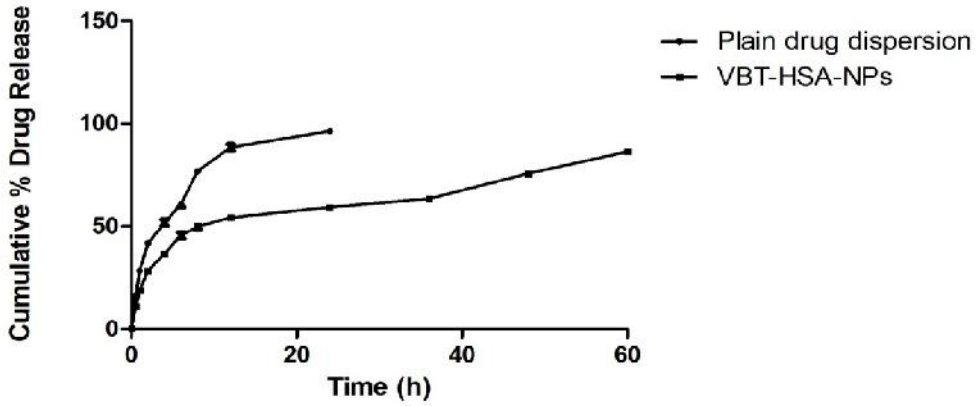

Figure 5. 27 *In vitro* drug release pattern

5.8.3.5 Stability of VBT HSA NPs

Stability study results of VBT-HSA-NPs for drug content and particle size are given in **Table 5.11.** Comparative changes in particle size with temperature during stability shown in **Figure 5.28.** It was observed that VBT-HSA-NPs were stable over the period of 6 months at 2-8°C and Room Temperature. The VBT-HSA-NPs showed physical stability for the period of 6 months at 2-8°C. The drug content at room temperature was found to decrease during storage and the particle size was also increased above 200 nm, which was not desirable. Hence, Room Temperature is not

suitable for storage of VBT-HSA-NPs while storage at 2 -8°C no significant difference was observed in the particle size and drug content of NPs after 6 months at refrigerated conditions indicating its suitability for storage at 2 -8°C.

Table 5. 13 Stability data of VBT-HSA-NPs at different temperature conditions.

Temperature Condition	Sampling Time (days)	Particle size in nm (Mean ± SD)	% Assay (Mean ± SD)
Initial	0	154.3 ± 4.72	99.78 ±0.078
Room Temp.	15	159.3 ± 3.84	99.56±0.024
	30	162.4 ± 5.32	99.24±0.065
	45	169.5 ± 4.84	98.89±0.056
	60	178.6 ± 3.72	98.67±0.054
	90	189.7 ± 3.86	98.12±0.046
	180	210.6 ± 4.56	97.86±0.062
2-8îC	15	155.1 ± 2.67	99.68±0.065
	30	156.4 ± 3.34	99.56±0.043
	45	160.8 ± 3.56	99.34±0.034
	60	162.3 ± 3.52	99.28±0.075
	90	165.4 ± 3.67	99.22±0.048
	180	167.8 ± 2.89	99.14±0.038

*** The experiment was performed in triplicate (n=3)**

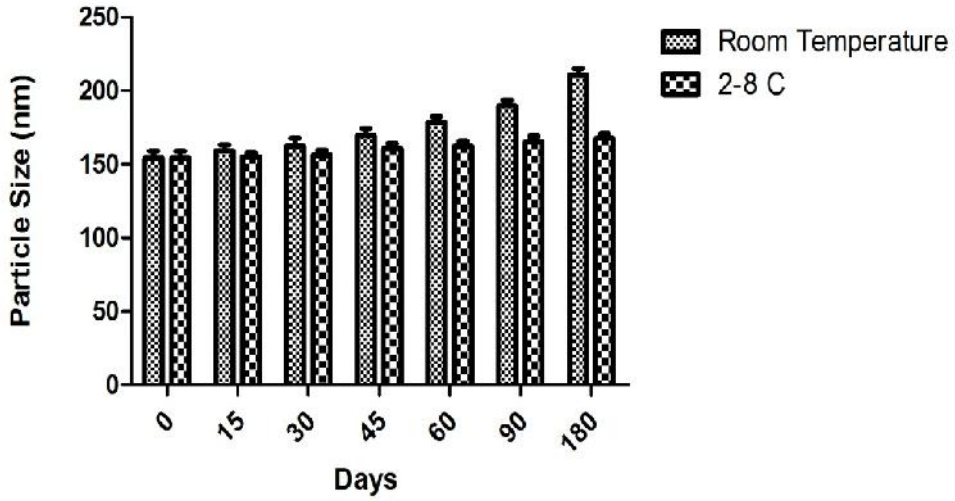

Figure 5. 28 Comparative changes in particle size with temperature during stability

5.9 Discussion

VBT-HSA-NPs were successfully prepared by desolvation method. In earlier study, the amount of the desolvating agent i.e. ethanol, in the desolvation process was found to control particle size, but the variability in size at a given ethanol amount was high in the condition of manual performance. Considering the high variability originated from manual addition of ethanol, a constant flow pump was used, which enabled a defined rate of ethanol addition in this study. The desolvation process determines whether albumin NPs with a suitable particles size could be prepared. The pH value of the albumin solution plays an important role in the desolvation process. The isoelectric point of HSA is pI = 5.3 indicate that the human serum has a positive charge below pI 5.3 and negative charge above pI 5.3 (16). At pH values around the pI, the NPs became unstable. In aqueous media, the pH of the sample is one of the most important factors that affect its zeta potential. If more alkali is added to the particles suspension with a negative zeta potential, the particles tend to acquire more negative charge. Maybe it's the reason why increasing pH values led to the increase of zeta potential absolute value. For the purpose of increasing the zeta potential and stability of the prepared NPs, 10 mM NaCl solution instead of water, was employed as the solvent of albumin, which could increase the ion concentration and electric conductivity of the solution. Furthermore, each parameter such as the albumin concentration, amount of vinorelbine, pH value and percentage of glutaraldehyde were optimized in order to achieve a colloidal system with well-defined physicochemical characteristics (17). The most efficient condition for this preparation would use the lowest mean particle size, and the highest entrapment efficiency. Optimum experimental condition was suggested by optimization software.

The particle sizes and zeta potential of optimized formulation were measured in triplicates and the results were 154.3±4.72 nm and -15.6±2.074 mV respectively. The % EE of VBT-HSA-NPs was found 75.24± 2.23%. The TEM images of the NPs revealed their regular spherical shape, as well as a range of diameters. This is much closer to the ideal particle size, which is between 100 and 200 nm. For particles larger than 200 nm, the phagocytic uptake is faster because of enhanced opsonization. Particles smaller than 100 nm are able to cross the fenestration of the hepatic sinusoidal endothelium, accumulate in the liver and have the tendency to unspecific uptake in all

tissues. In DSC thermogram, VBT-HSA-NPs no melting process was observed which indicates that NPs were nanostructured and non-crystalline.

The *in vitro* drug release studies of VBT-HSA-NPs were carried out in trypsin phosphate buffered saline (pH 7.4) by diffusion method for 60 hr and the results were compared by different kinetic models. An initial burst of more than 60% of the plain VBT in first 6 hr was observed then a slow release up to 24 hr. A cumulative release reached 96% for plain VBT, while VBT-HSA-NPs showed a slow release of drug up to 60 hr, releasing approximately 86% of VBT. It is evident that the sustained release of drug from VBT-HSA-NPs will provide a better therapeutic efficacy than plain VBT. After application of different drug release kinetics models, it was observed that the VBT-HSA-NPs followed the Korsmeyer Peppas model because R^2 value (0.9379) which was nearer to 1 and having n value of 0.3798 indicating that drug transport mechanism is Fickian diffusion. Stability study results of VBT-HSA-NPs for drug content and particle size are evaluated and it was observed that VBT-HSA-NPs were stable over the period of 6 months at 2-8°C. Based on these results it was concluded that optimized VBT-HSA-NPs are suitable for further targeting studies.

5.10 References

1. Storp B, Engel A, Boeker A, Ploeger M, Langer K. Albumin nanoparticles with predictable size by desolvation procedure. J Microencapsul. 2012;29(2):138-46.
2. Yedomon B, Fessi H, Charcosset C. Preparation of Bovine Serum Albumin (BSA) nanoparticles by desolvation using a membrane contactor: a new tool for large scale production. Eur J Pharm Biopharm. 2013 Nov;85(3 Pt A):398-405.
3. Lamprecht A, Ubrich N, Hombreiro Perez M, Lehr C, Hoffman M, Maincent P. Influences of process parameters on nanoparticle preparation performed by a double emulsion pressure homogenization technique. Int J Pharm. 2000 Mar 10;196(2):177-82.
4. Carter DC, Ho JX. Structure of serum albumin. Adv Protein Chem. 1994;45:153-203.
5. Kouchakzadeh H, Shojaosadati SA, Maghsoudi A, Vasheghani Farahani E. Optimization of PEGylation conditions for BSA nanoparticles using response surface methodology. AAPS PharmSciTech. 2010 Sep;11(3):1206-11.
6. Delf Loveymi B, Jelvehgari M, Zakeri-Milani P, Valizadeh H. Statistical Optimization of Oral Vancomycin-Eudragit RS Nanoparticles Using Response Surface Methodology. Iran J Pharm Res. 2012 Fall;11(4):1001-12.
7. Li L, Zhao X, Yang C, Hu H, Qiao M, Chen D. Preparation and optimization of doxorubicin-loaded albumin nanoparticles using response surface methodology. Drug Dev Ind Pharm. 2011 Oct;37(10):1170-80.
8. Bhupinder S, Rajiv K, Ahuja N. Optimizing Drug Delivery Systems Using Systematic “Design of Experiments.” Part I: Fundamental Aspects. Critical Reviews™ in Therapeutic Drug Carrier Systems. 2004;22(1):27-105.
9. Ratcliffe E, Hourd P, Guijarro-Leach J, Rayment E, Williams DJ, Thomas RJ. Application of response surface methodology to maximize the productivity of scalable automated human embryonic stem cell manufacture. Regen Med. 2013 Jan;8(1):39-48.
10. Elmizadeh H, Khanmohammadi M, Ghasemi K, Hassanzadeh G, Nassiri-Asl M, Garmarudi AB. Preparation and optimization of chitosan nanoparticles and magnetic chitosan nanoparticles as delivery systems using Box-Behnken statistical design. J Pharm Biomed Anal. 2013 Jun;80:141-6.

11. Box GEP, Wilson K. On the experimental attainment of optimum conditions. J Roy Stat Soc. 1951;13:1-45.
12. Yadav KS, Sawant KK. Formulation optimization of etoposide loaded PLGA nanoparticles by double factorial design and their evaluation. Curr Drug Deliv. 2010 Jan;7(1):51-64.
13. Kumar A, Sawant KK. Application of multiple regression analysis in optimization of anastrozole-loaded PLGA nanoparticles. J Microencapsul. 2014;31(2):105-14.
14. Zhang JY, He B, Qu W, Cui Z, Wang YB, Zhang H, et al. Preparation of the albumin nanoparticle system loaded with both paclitaxel and sorafenib and its evaluation in vitro and in vivo. J Microencapsul. 2011;28(6):528-36.
15. Calvo P, Vila-Jato JL, Alonso M. Comparative in vitro evaluation of several colloidal systems, nanoparticles, nanocapsules and nanoemulsions as ocular drug carrier. J Pharm Sci. 1996;85:530-6.
16. Lin W, Coombes AG, Davies MC, Davis SS, Illum L. Preparation of sub-100 nm human serum albumin nanospheres using a pH-coacervation method. J. Drug Target. 1993;1:237-43.
17. Langer K, Balthasar S, Vogel V, Dinauer N, von Briesen H, Schubert D. Optimization of the preparation process for human serum albumin (HSA) nanoparticles. Int J Pharm. 2003;257:169-80.